Bioorganic & Medicinal Chemistry 17 (2009) 5834–5856

Contents lists available at ScienceDirect

Bioorganic & Medicinal Chemistry

journal homepage: www.elsevier.com/locate/bmc

Rational design, synthesis and characterization of potent, non-peptidic Smac mimics/XIAP inhibitors as proapoptotic agents for cancer therapy

Pierfausto Seneci [a,b,*], Aldo Bianchi [b], Cristina Battaglia [b,c], Laura Belvisi [a,b], Martino Bolognesi [d], Andrea Caprini [b], Federica Cossu [d], Elena de Franco [b], Marilenia de Matteo [b], Domenico Delia [e], Carmelo Drago [b], Amira Khaled [b], Daniele Lecis [e], Leonardo Manzoni [b,f], Moira Marizzoni [b], Eloise Mastrangelo [d], Mario Milani [d], Ilaria Motto [b], Elisabetta Moroni [b], Donatella Potenza [a,b], Vincenzo Rizzo [b], Federica Servida [g], Elisa Turlizzi [h], Maurizio Varrone [h], Francesca Vasile [b], Carlo Scolastico [a,b]

[a] *Dipartimento di Chimica Organica e Industriale, Università degli Studi di Milano, Via Venezian 21, I-20133 Milan, Italy*
[b] *Centro Interdisciplinare di Studi Biomolecolari e Applicazioni Industriali (CISI), Università degli Studi di Milano, Via Fantoli 16/15, I-20138 Milan, Italy*
[c] *Dipartimento di Scienze e Tecnologie Biomediche, Università degli Studi di Milano, Via Fratelli Cervi 93, 20090 Segrate (MI), Italy*
[d] *Dipartimento di Scienze Biomolecolari e Biotecnologie e CNR-INFM, Università degli Studi di Milano, Via Celoria 26, I-20133 Milan, Italy*
[e] *Dipartimento di Oncologia Sperimentale, Istituto Nazionale dei Tumori (INT), Via Venezian 1, I-20133 Milan, Italy*
[f] *Istituto di Scienze e Tecnologie Molecolari (ISTM), Consiglio Nazionale delle Ricerche (CNR), Via Fantoli 16/15, I-20138, Milan, Italy*
[g] *Fondazione Matarelli, Dipartimento di Farmacologia, Chemioterapia e Tossicologia Medica, Università degli Studi di Milano, Via Vanvitelli 32, I-20129 Milan, Italy*
[h] *SienaBiotech S.p.A., Via Fiorentina 1, I-53100, Siena, Italy*

ARTICLE INFO

Article history:
Received 21 May 2009
Revised 1 July 2009
Accepted 5 July 2009
Available online 10 July 2009

Keywords:
XIAP
Smac
Apoptosis
Oncology
Rational drug design
Crystallography
NMR
Medicinal chemistry

ABSTRACT

Novel proapoptotic Smac mimics/IAPs inhibitors have been designed, synthesized and characterized. Computational models and structural studies (crystallography, NMR) have elucidated the SAR of this class of inhibitors, and have permitted further optimization of their properties. In vitro characterization (XIAP BIR3 and linker-BIR2–BIR3 binding, cytotox assays, early ADMET profiling) of the compounds has been performed, identifying one lead for further in vitro and in vivo evaluation.

1. Introduction

The apoptotic process of programmed cell death (PCD) and dysfunctions in its regulation in a variety of human pathologies, among which cancer[1,2] and neurodegenerative diseases,[3] have become the focus of extensive pharmaceutical research. A variety of pathways have been reported as leading to PCD. Among them, the extrinsic or death receptor-dependent path[4,5] and the intrinsic or mitochondrial path,[4,6] both of them caspase-dependent; and a variety of caspase-independent pathways, such as apoptosis inducing factor (AIF)-dependent apoptosis.[7]

In such a heterogeneous and complex scenario, hitting more than one of the putative significant targets with a given lead should maximize the chances of therapeutic success. Thus, we focused on targeting molecular entities involved both in the extrinsic and intrinsic caspase-dependent pathways.

The family of Inhibitor of Apoptosis Proteins (IAPs)[8,9] is characterized by the presence of one or more Baculovirus IAP Repeat (BIR) domains. Since the discovery of the first viral *iap* gene and its linkage with apoptosis,[10] IAPs were considered putative targets for pro-apoptotic drugs in oncology. The assumption of a common anti-apoptotic mechanism for IAPs through interference with caspase-dependent pathways[11] has been proven only partially correct for some human IAPs,[12,13] but their interest as oncology targets related to PCD has not been seriously challenged.

* Corresponding author. Tel.: +39 02 50320914; fax: +39 02 50320945.
E-mail address: pierfausto.seneci@unimi.it (P. Seneci).

0968-0896/$ - see front matter © 2009 Elsevier Ltd. All rights reserved.
doi:10.1016/j.bmc.2009.07.009

Surely, the most caspase-connected human IAP is the X-Inhibitor of Apoptosis Protein[14,15] (XIAP). XIAP is capable of binding caspase 9 (the initiator caspase) and both caspases 3 and 7 (the executioner caspases).[16] XIAP binding prevents activation of caspases and, consequently, prevents cells from entering PCD. Another protein released from mitochondria, the Second Mitochondria-derived Activator of Caspases (Smac)[17]/Direct IAp Binding protein with LOw pI (DIABLO)[18] is able to bind XIAP as a dimer[19] on the same binding sites of caspase 9 (BIR3 domain).[20–22] Smac interferes also with the XIAP binding site of caspases 3 and 7 (linker-BIR2 domain),[23] thus promoting both the extrinsic and intrinsic PCD paths. The delicate balance of this binding equilibrium is altered in various diseases; for example, several tumour cell lines show overexpression of XIAP and, consequently, a caspase-dependent resistance to enter PCD.[24,25] Thus, XIAP inhibition via Smac mimics' binding is considered a validated mechanism for intervention in cancer therapy;[26] moreover, structurally related human IAP family members such as cIAP1[27] and cIAP2,[28] other popular oncology targets,[29] can also be targeted by Smac mimics.

Recently several authors have shown how small monomeric Smac mimics/XIAP inhibitors such as **1a** and **1b**, inspired by the Smac N-terminal AVPI sequence and built on the 1-aza-2-oxo-3-aminobicyclo[5.3.0]decane-10-carboxylic acid scaffold **2**, can bind XIAP on its BIR3 domain with sub-micromolar potency, and have an effect on apoptosis in tumour cells.[30,31] Here we report a structure-driven approach to potent, monomeric Smac mimics/XIAP inhibitors of general formula **I**.[32]

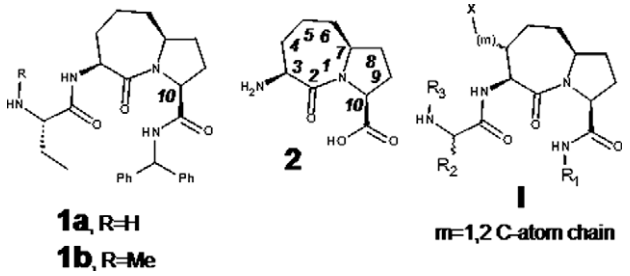

The introduction of an appropriate 4-substitution on the 1-aza-2-oxobicyclo[5.3.0]decane scaffold (i.e., (m)X = CH_2OH as in top left, and (m)X = CH_2NH_2 as in top right, Fig. 1), when compared with known **1a**,**b**[30,31] and other 4-unsubstituted analogues, establishes novel molecular interactions with the binding sites on XIAP and contributes to an overall improvement in the 'drug-like' profile (i.e., solubility, penetration through biological membranes) of our Smac mimics/XIAP inhibitors. Computational, NMR and X-ray data, and the resulting structural information acquired, have contributed to the establishment of a preliminary SAR for XIAP inhibitors, and to the design of optimized analogues.

2. Results and discussion

2.1. Computational studies

Some of us recently reported[33,34] an innovative synthesis strategy to access compounds of general formula **I**, which differ from reported structures for an additional 4-substitution on the 1-aza-2-oxobicyclo[5.3.0]decane scaffold. Having secured synthetic access to such structures, we decided to ascertain if appropriate substituents on the 4-position could be reconduced to advantageous interactions with members of the IAP family, and with XIAP in particular. A structure-based approach, based on a computational model of the AVPI-binding sites of the BIR3 domain of XIAP and on data from NMR and X-ray crystallography, was conceived to understand and optimize the effects of 4-substitutions on the 1-aza-2-oxobicyclo[5.3.0]decane nucleus.

A docking approach has been set up starting from the high resolution crystal structure of the Smac/BIR3 complex (PDB code 1G73).[21] The Glide[35] docking protocol reproduced the crystallographic binding mode of AVPI in BIR3, and the measured BIR3 binding affinity trend of a previously reported[30] training set of Smac mimics including **1a**. The validated docking protocol was applied to a small library of ligands of general formula **I** (most promising structures shown in Fig. 1).

Nitrogen and/or oxygen-containing functional groups in position 4 (e.g., amines, alcohols, amides and ureas) and aromatic lipo-

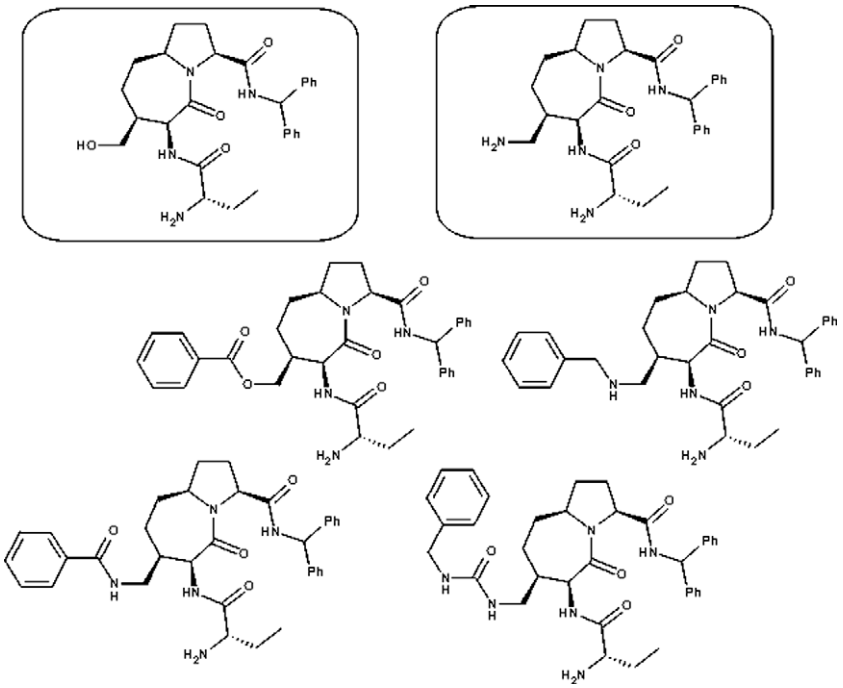

Figure 1. Prioritized 4-substitutions.

philic extensions on the 4-arm (e.g., phenyl ester and amide, benzyl amine or urea, Fig. 1) resulted to be privileged substitutions. In particular, 4-substituted compounds in Figure 1 showed an AVPI-like binding mode and additional hydrophobic contacts with the protein involving the azabicycloalkane scaffold and the phenyl rings. Furthermore, most of them seemed to establish additional interactions through their 4-side chains, such as hydrogen bonds through the interaction with the Thr308 and/or the Asp309 BIR3 residues (shown for the hydroxy compound, Fig. 2).

These encouraging theoretical findings prompted us to synthesize a medium-sized array of 4-substituted 1-aza-2-oxobicyclo[5.3.0]decanes of general formula **II**, where X is a substituted nitrogen atom or a substituted oxygen atom. Thus, we constantly kept the (*S*)-ethylglycine and the diphenylamino 'best' substitutions on the 3-NH_2 and 10-COOH groups in scaffold **2**, targeting compounds of formula **IIa**.

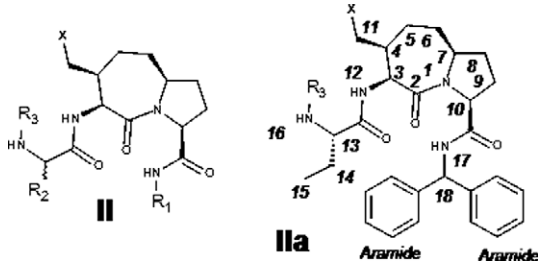

2.2. Synthesis—structures IIa

At first, we prepared the 4-substituted primary alcohol **3a** and primary amine **4a** (Scheme 1). Briefly, compound **5**[34] was transesterified (HCl, MeOH), hydrogenated (Pd/C, 5 atm) and coupled with BocNHAbuOH (HOBt, EDC, DIPEA) to give **6a**. Ester hydrolysis (LiOH) and coupling with diphenylaminomethane (HOBt, EDC, DIPEA) gave **7a**. The N-protected 4-CH_2OH compound **7a** was then transformed into the 4-CH_2NH_2 compound **9a** via mesylation (MsCl, TEA), azide displacement (NaN_3) to give the N-protected 4-CH_2N_3 compound **8a**, and Staudinger reduction. *N*-Boc protected compounds **7a** and **9a** were deprotected (HCl, MeOH) to give, after preparative HPLC purification, pure compounds **3a** and **4a** as hydrochloride salts (overall unoptimized yield: 35%, **3a** and 8%, **4a**).

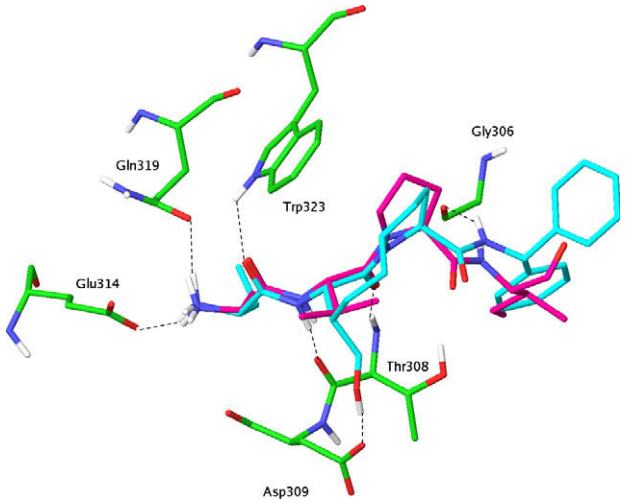

Figure 2. Docking best pose of the 4-CH_2OH compound (cyan) into the crystallographic (1G73) BIR3 binding site (protein residues involved in hydrogen bond interactions are labelled; C atoms in green, N in blue and O in red) overlaid on the AVPI-bound conformation (magenta). Non polar hydrogens hidden for better visual representation, intermolecular hydrogen bonds visible (black dashed lines).

Recently it was reported[28] that the *N*-methyl 4-unsubstituted compound **1b** retains similar potency on cell-free XIAP binding assays, while largely improving its cytotoxicity against cancer cells with respect to **1a**. We thus prepared the N-methylated 4-CH_2OH and 4-CH_2NH_2 compounds **3b** and **4b** from **5** (overall unoptimized yield: 39%, **3b** and 6%, **4b**) as seen for compounds **3a** and **4a**, simply replacing BocNHAbuOH with BocN(Me)AbuOH and going through intermediates **6b**–**7b** (**3b**) and **6b**–**10b** (**4b**, Scheme 1). Due to the instability of **9b** in acidic Boc deprotection conditions, **4b** was obtained via Boc deprotection (**10b**) and final azide reduction (H_2, Pd/C).

Compounds **7a**, **8a** and **9a** were used to access other 4-substituted Smac mimics. Most compounds were obtained as pure materials after final preparative HPLC purification. The synthesis of compounds prepared from N-protected alcohol **7a** and N-protected azide **8a** is reported in Scheme 2.

The N-protected alcohol **7a** was acylated (RCOCl, DMAP) to give *N*-Boc protected **11a**,**b**, and deprotected (TFA, CH_2Cl_2) to provide the esters **12a**,**b** as TFA salts (overall unoptimized yield: 46%, **12a** and 85%, **12b**). The N-protected azide **8a** was deprotected (HCl, MeOH) to provide the azide **10a** as a hydrochloride salt in 45% unoptimized yield. It was also reacted in 'click chemistry' conditions (1-pentynyl-3-ol, $Cu(OAc)_2$, sodium ascorbate) to give the triazolyl alcohol **14a** as a hydrochloride salt after deprotection of *N*-Boc protected **13a** (HCl, MeOH) in overall 58% unoptimized yield. Finally, it was guanylated (guanylating agent, LiOH, Ph_3P) to yield the guanidino compound **16a** after deprotection of *N*-Boc protected **15a** (HCl, MeOH) in overall 31% unoptimized yield.

The N-protected primary amine **9a** was used to obtain several classes of compounds (Schemes 3 and 4).

Secondary amines **18a**,**b** were prepared (overall unoptimized yield: 71%, **18a** and 76%, **18b**) by reductive amination (RCHO, $NaBH(OAc)_3$) to give *N*-Boc protected compounds **17a**,**b**, and deprotection (HCl, MeOH). Both *N*-Boc protected secondary amines were also converted to tertiary amines **20a**,**b** (from **17b**, overall unoptimized yield from **9a**: 70%, **20a** and 68%, **20b**) and **20c** (from **17a**, overall unoptimized yield from **9a**: 47%) by reductive amination (RCHO, $NaBH(OAc)_3$) and deprotection (HCl, MeOH) (Scheme 3).

Carboxylic amides **22a–c** were prepared (overall unoptimized yield: 61%, **22a** , 88%, **22b** and 71%, **22c**) either from carboxylic acids (**22a**: RCOOH, EDC, HOBt, DIPEA) or from acyl chlorides (**22b**,**c**: RCOCl, pyridine), after final deprotection of *N*-Boc protected compounds **21a–c** (HCl, MeOH) (Scheme 4). Similarly, sulfonamides **24a**,**b** were prepared (overall unoptimized yield: 67%, **24a** and 74%, **24b**) from sulfonyl chlorides (RSO_2Cl, K_2CO_3), after final deprotection of *N*-Boc protected compounds **23a**,**b** (HCl, MeOH). N,N′-Substituted ureas **26a**,**b** (overall unoptimized yield: 81%, **26a** and 93%, **26b**) and thioureas **26c**,**d** (overall unoptimized yield: 87%, **26c** and 83%, **26d**) were prepared by the addition of the corresponding isocyanates or isothiocyanates (RCNX, DIPEA), followed by deprotection of *N*-Boc protected compounds **25a–d** (HCl, MeOH). Finally, the N′-unsubstituted urea **28a** (overall 66% unoptimized yield) and thiourea **28b** (overall 56% unoptimized yield) were prepared by addition of the corresponding benzoylisocyanate or isothiocyanate (PhCONCX, DIPEA), followed by basic (K_2CO_3, MeOH) and acidic (HCl, MeOH) deprotection of *N*-Boc protected compounds **27a**,**b** (HCl, MeOH).

2.3. Biophysical characterization—structures IIa

In parallel with our synthetic efforts, we investigated the influence of the 4-substitution in Smac mimics/IAPs inhibitors of general formula **IIa** by using some popular biophysical methods.

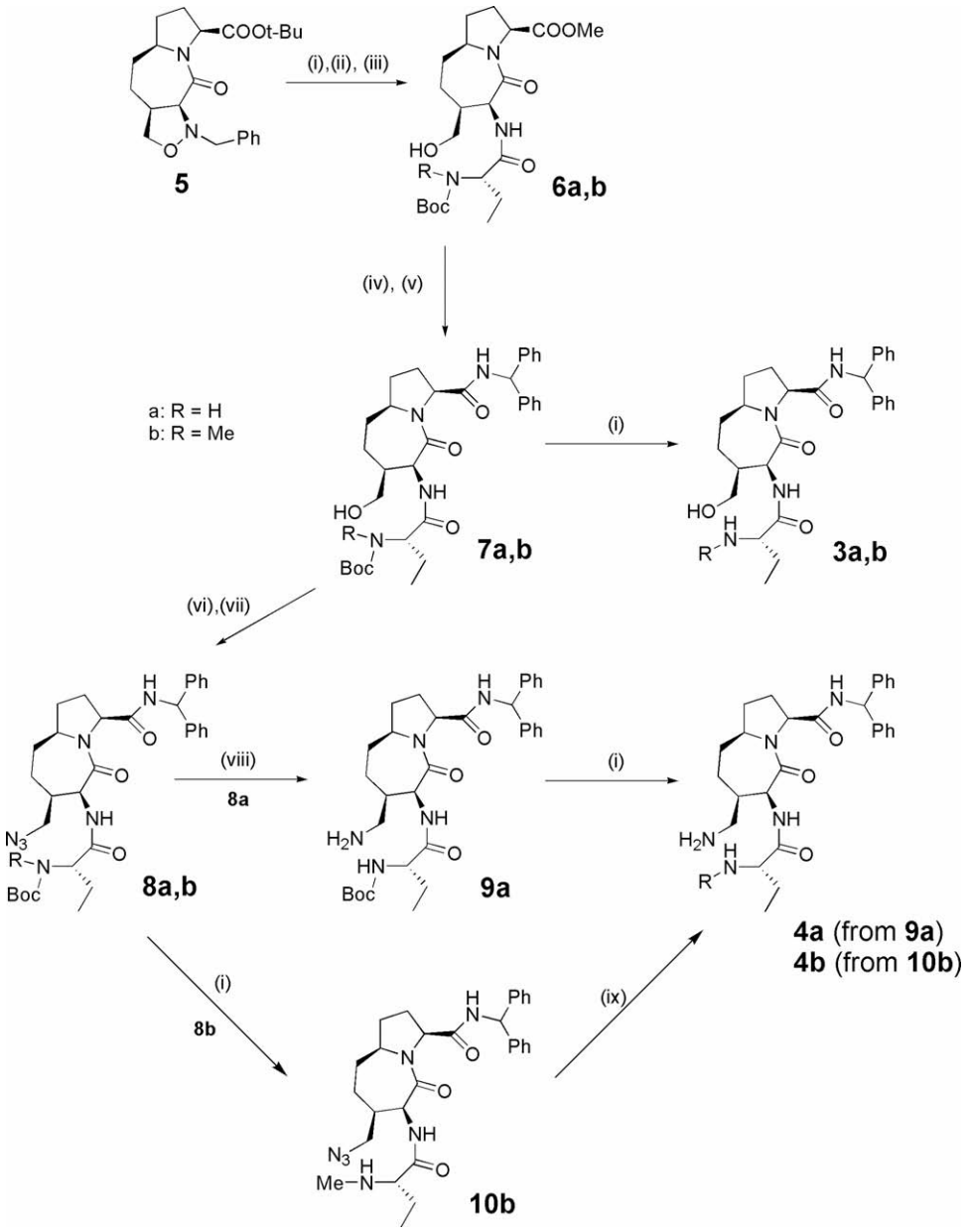

Scheme 1. Reagents and conditions: (i) 3 N HCl in MeOH, rt; (ii) H_2, Pd/C, 5 atm, rt; (iii) BocNHAbuOH (a) or BocN(Me)AbuOH (b), HOBt, EDC·HCl, DIPEA, CH_2Cl_2, rt; (iv) LiOH, 1,4-dioxane, rt; (v) Ph_2CHNH_2, HOBt, EDC·HCl, DIPEA, CH_2Cl_2, rt; (vi) MsCl, TEA, CH_2Cl_2, rt; (vii) NaN_3, DMF, 80 °C; (viii) Me_3P, H_2O/CH_2Cl_2, rt; (ix) H_2, Pd/C, H_2O/1,4-dioxane 1:1, rt.

Namely, we submitted a few compounds (together with the standard compound **1a**[30]) to extensive NMR and X-ray characterization in presence of either full length XIAP, and some of its BIR domains responsible for caspase and Smac binding.

As to crystallography, while co-crystals with **1a** were not obtained, both compounds **3a** and **4a** provided good co-crystals with the BIR3 domain of XIAP. Up to now, we could not obtain any co-crystal of either **1a**, **3a** or **4a** with the BIR2 XIAP domain. The BIR3-inhibitor crystals of **3a** and **4a** were thoroughly characterized through X-ray crystallography (3D structures refined at 2.7 and 2.5 Å resolution, respectively).[36] The compounds bind to the AVPI site, establishing specific hydrogen bonds and contacts. The primary alcohol **3a** shows a binding mode with minimal changes with respect to the BIR3–AVPI complex, although an additional hydrogen bond stems from the interaction of the 4-CH_2OH group with Thr308 of BIR3[37] (data not shown). Remarkably, the binding mode of the primary amine **4a** with BIR3 shows an overall shift (1.5 Å on average, relative to **3a**) towards the Asp309 residue, with concomitant loss of hydrogen bonds and hydrophobic interactions. The shift is mostly due to the appearance of a novel hydrogen bond/salt bridge interaction between the positively charged 4-CH_2NH_2 group in **4a** and the highly mobile Asp309 residue[36] (Fig. 3).

As to NMR, saturation transfer difference (STD-NMR)[38] was used to highlight binding interactions between **1a**, **3a**, **4a**, **16a** and **18b** as small ligands, and recombinant XIAP BIR3 (primary Smac binding site, caspase 9 binding site), the construct linker-BIR2–BIR3 (including the secondary Smac binding site linker-BIR2, caspases 3 and 7 binding site) and full length XIAP as targets. Using STD, only the ligand protons interacting with the target are visible in the NMR spectrum (see formula **IIa** for proton numbering), thus identifying the ligand binding regions. While we could not obtain and use the linker-BIR2 construct per se, we reasoned that any additional proton–ligand interaction observed for a given small ligand in presence of the construct linker-BIR2–BIR3 (or of

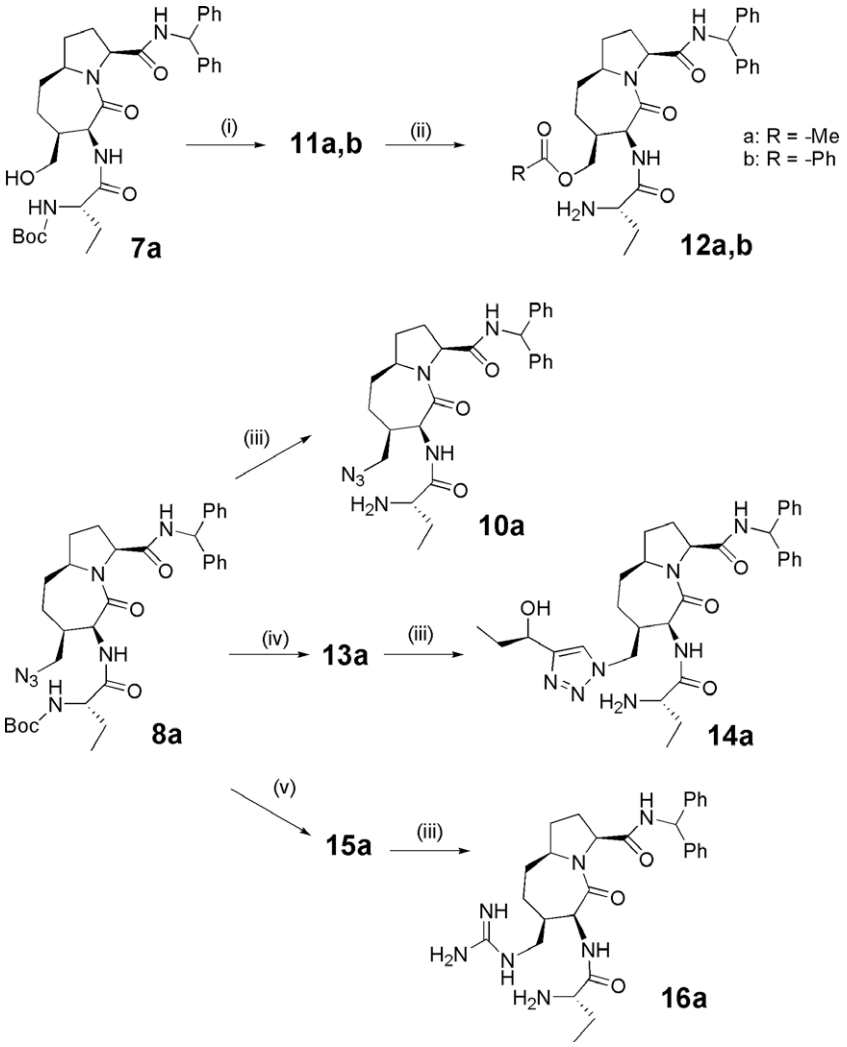

Scheme 2. Reagents and conditions: (i) RCOCl, DMAP, CH_2Cl_2, rt; (ii) TFA, CH_2Cl_2, rt; (iii) 3 N HCl in MeOH, rt; (iv) 1-pentynyl-3-ol, sodium ascorbate, $Cu(OAc)_2$, H_2O/*t*-BuOH, rt; (v) *N*,*N*′-bis-Boc-1-guanylpyrazole, LiOH, Ph_3P, H_2O/THF, rt.

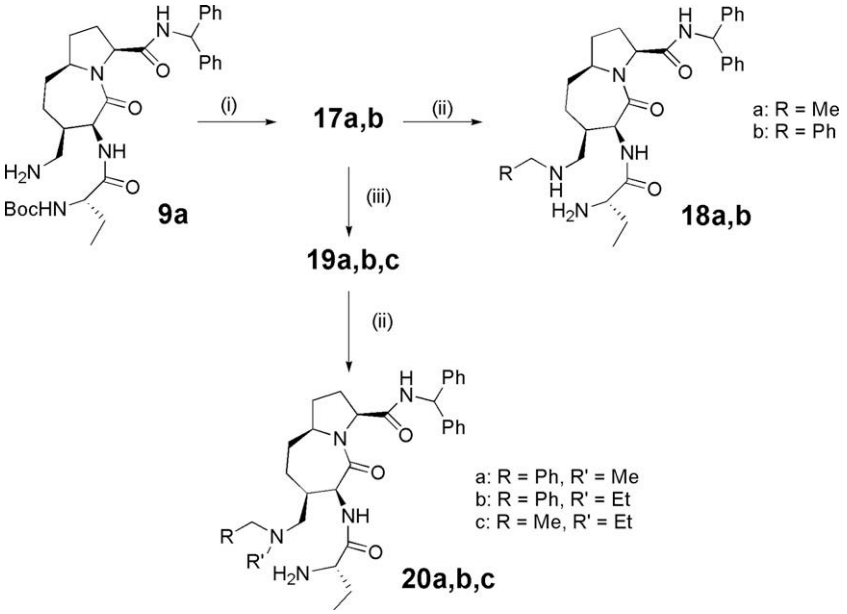

Scheme 3. Reagents and conditions: (i) RCHO, $NaBH(OAc)_3$, CH_2Cl_2, rt; (ii) 3 N HCl in MeOH, rt; (iii) RCHO, $NaBH(OAc)_3$, AcOH, CH_2Cl_2, rt.

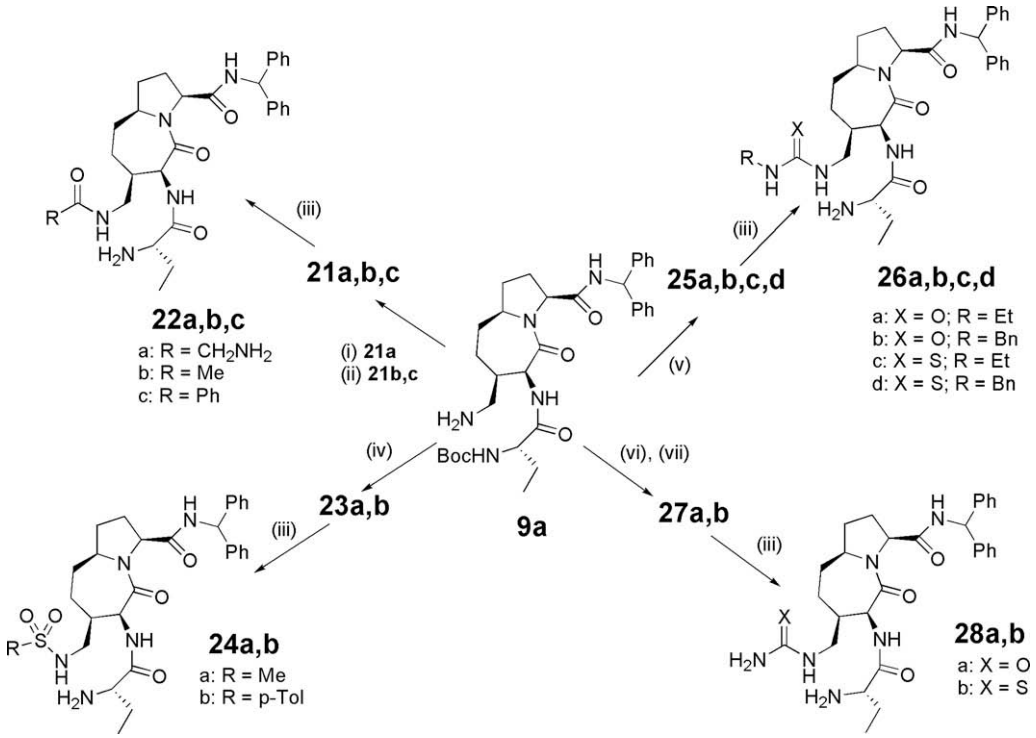

Scheme 4. Reagents and conditions: (i) RCOOH, EDC, HOBt, DIPEA, CH_2Cl_2, rt; (ii) RCOCl, pyridine, CH_2Cl_2, rt; (iii) 3 N HCl in MeOH, rt; (iv) RSO_2Cl, K_2CO_3, CH_2Cl_2, rt; (v) RCNX, DIPEA, CH_2Cl_2, rt; (vi) PhCOCNX, DIPEA, CH_2Cl_2, rt; (vii) K_2CO_3, MeOH, rt.

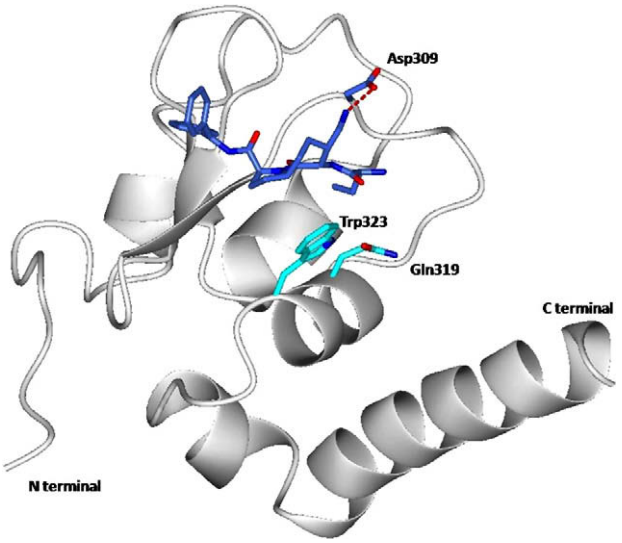

Figure 3. X-ray crystal structure of **4a** (blue skeletal model) and XIAP BIR3 (grey ribbon): the interaction between the 4-CH_2NH_2 group and Asp309 is visible in the upper part. N- and C-terminal ends of the BIR3 domain are labeled.

full length XIAP), and absent in presence of the BIR3 domain alone should indicate an interaction targeted to the linker-BIR2 binding site.

The spectra of reference compound **1a** (Fig. 4) in presence of BIR3 (lane A) and of full length XIAP (lane B) show a similar interaction pattern, including protons in the bicyclic scaffold (e.g., H_3 and H_{10}), on the diphenylamide moiety (e.g., the aromatic protons) and on the ethylglycine moiety (e.g., H_{13}, H_{15}).

The spectra of **3a** (Fig. 5) in presence of various binding partners suggest different binding interactions of 4-substituted 1-aza-2-oxobicyclo[5.3.0]decanes with BIR2 and BIR3 domains. The diphenylamido (7.3 ppm-Ar amide, 6.0 ppm-H_{18}, strong interaction) and the ethylglycine moiety (0.9 ppm-H_{15}) both interact with BIR3 (lane A), while no interaction with any scaffold proton is detectable. Conversely, both the construct linker-BIR2–BIR3 (lane B) and full length XIAP (lane C) show a strong interaction with the 4-substituted 1-aza-2-oxobicyclo[5.3.0]decane scaffold itself (e.g., 4.0 ppm-H_7, 3.6 ppm-H_{11}/4-substitution), likely due to the linker-BIR2 domain.

Primary amine **4a**, when compared with **3a**, shows only a weak interaction of the ethylglycine moiety with BIR3 (data not shown) most likely due to a shift in the BIR3 binding site in agreement with previously described X-rays evidence. Guanidine **16a** (data not shown) does not bind at all with BIR3, while benzylamine **18b** (Fig. 6) has an interaction profile with BIR3 comparable with **3a** (lane A). Namely, we observe interactions with Ar amide (7.3 ppm), H_{18} (6.0 ppm) and H_{15} (0.9 ppm) protons; for the first time we also observe an interaction between the BIR3 domain and the lipophilic part of the 4-substituent (7.4 ppm-benzyl Ar). Interactions between the *N*-benzyl 4-substitution of **18b** and XIAP BIR3 could also be observed within our computational experiments (i.e., proximity of the benzyl in **18b** with the side chain of Thr308, Fig. 7; favourable van der Waals contacts with the side chain of Asp309, Lys311 or Trp323 in other docking poses, data not shown).

4-Unsubstituted 1-aza-2-oxobicyclo[5.3.0]decanes, such as **1a**, seem to interact with the two XIAP-caspase binding sites similarly. Compounds **3a**, **4a**, **16a** and **18b** behave as **1a** in terms of binding with the linker-BIR2–BIR3 construct, sometimes showing additional interactions with 4-substituents. Namely, alcohol **3a** (3.6 ppm-H_{11}/4-substitution, lane B, Fig. 5) and benzylamine **18b** (7.4 ppm-benzyl Ar, lane B, Fig. 6) show such interactions, while small, charged 4-substituents (primary amine **4a**, guanidine **16a**) do not interact with linker-BIR2–BIR3. Conversely, substitution in 4 appears to prevent the interactions of scaffold protons and to modulate the interactions of the ethylglycine moiety with BIR3

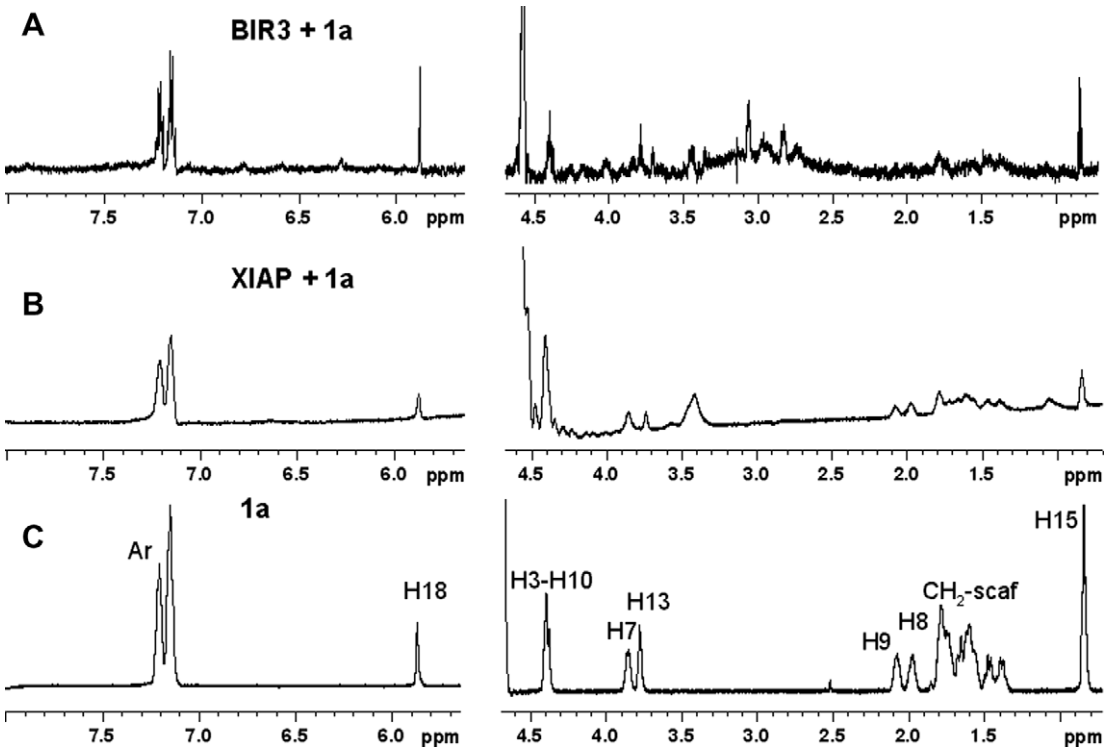

Figure 4. STD-NMR spectra of compound **1a** with BIR3 (A), full length XIAP (B) and as such (C).

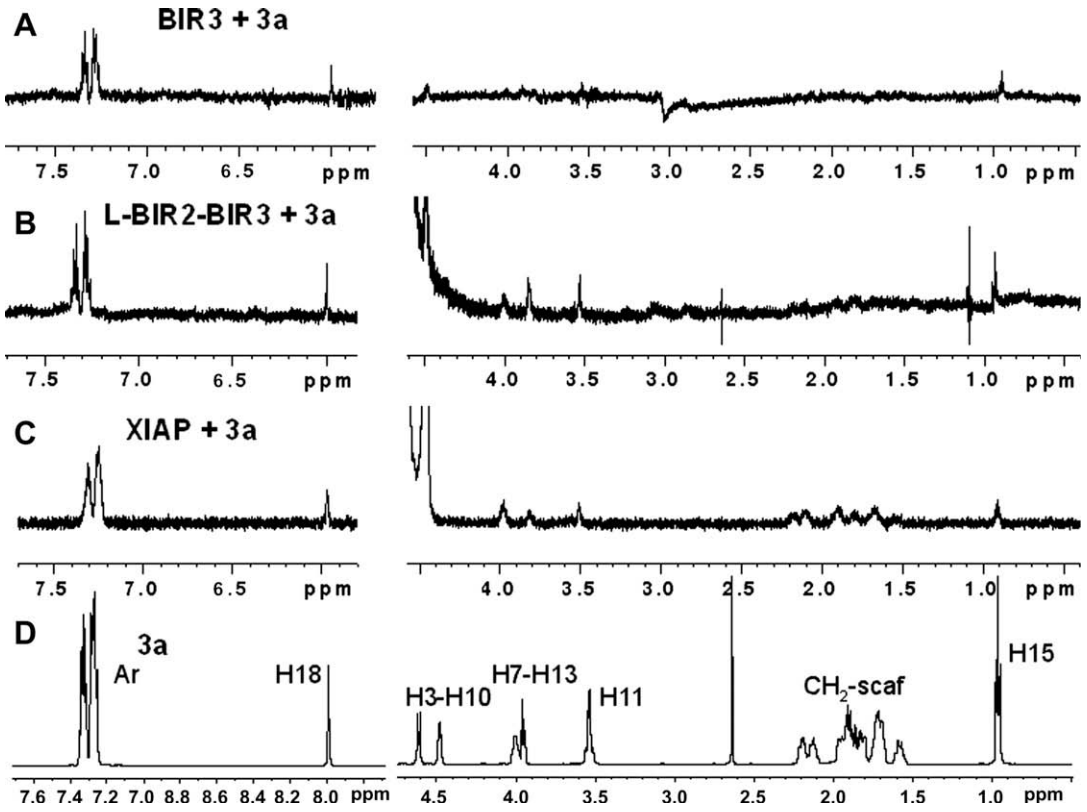

Figure 5. STD-NMR spectra of compound **3a** with BIR3 (A), linker BIR2–BIR3 (B), full length XIAP (C) and as such (D).

(**3a**,**18b** > **4a** > **16a**), thus differentiating our small ligands in terms of binding properties on different caspase binding domains. Ongoing and future STD–NMR experiments should clarify the impact of differential BIR2 and BIR3 binding modes for our small ligands on their biological activity, and to establish a robust SAR for further 4-substitutions.

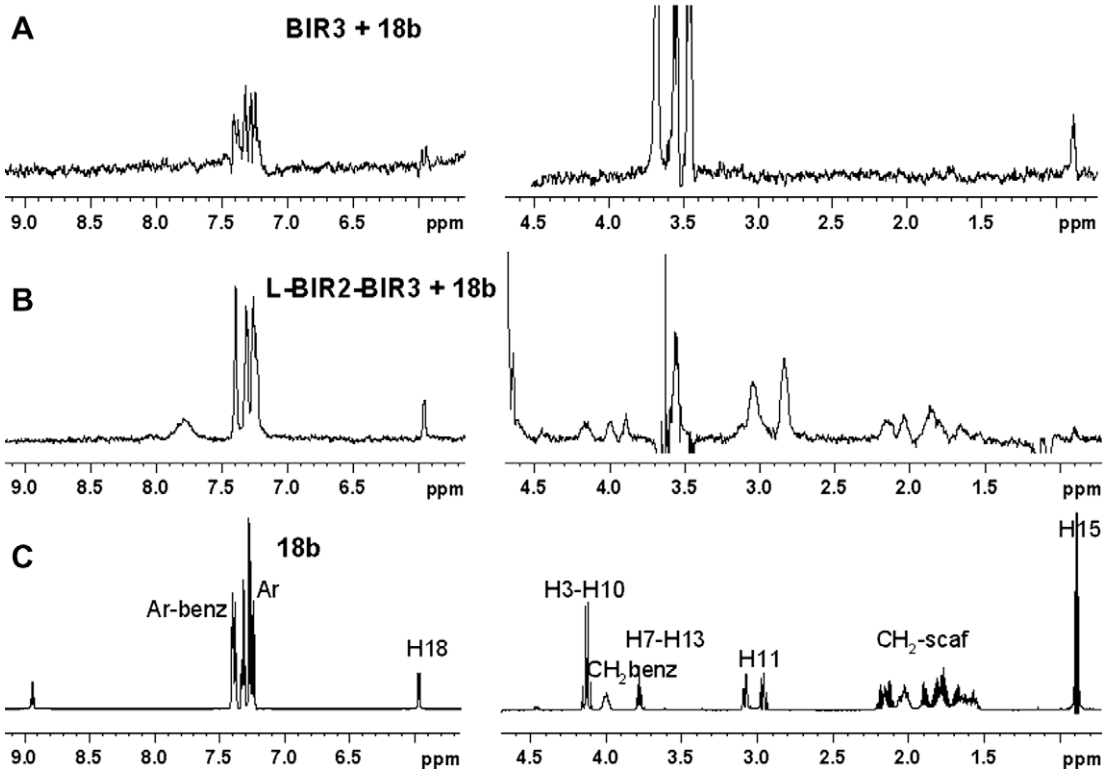

Figure 6. STD-NMR spectra of compound **18b** with BIR3 (A), linker-BIR2–BIR3 (B) and as such (C).

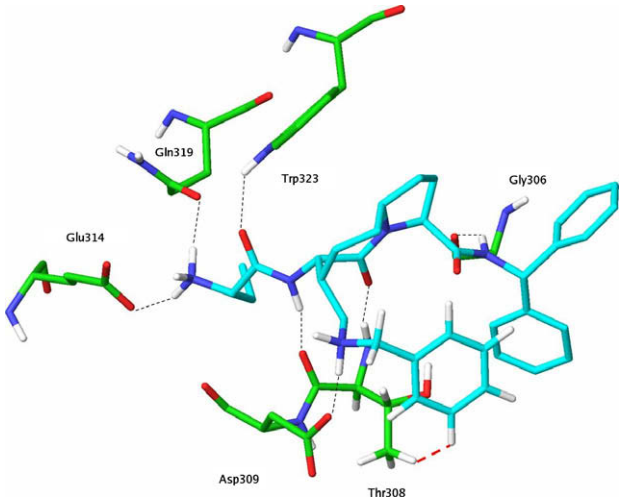

Figure 7. Docking best pose of **18b** (cyan) into the crystallographic (1G73) BIR3 binding site (protein residues involved in hydrogen bond interactions are labeled; C atoms are shown in green, N in blue, and O in red). Intermolecular hydrogen bonds are indicated as black dashed lines. Non polar hydrogens of Thr308 side chain and of the 4-CH_2NHCH_2Ph group in **18b** are shown to display van der Waals contacts (i.e., dashed red line, H–H distance = 3.0 Å).

Crystallographic data suggested a modest elongation of the scaffold's arm in **4a** to optimize the interaction between the 4-CH_2NH_2 and Asp309, without causing the shift of the ligand molecule observed for **4a** with associated loss of stabilizing interactions.[36] Thus, 4-elongated compounds with an additional CH_2 unit between position 4 on the scaffold and an ***X*** substituent, where ***X*** is a substituted nitrogen atom or a substituted oxygen atom, were targeted.

2.4. Synthesis, computational and biophysical characterization—elongated structures

In accordance with suggestions from crystallography, we first aimed to primary amine (R = $CH_2CH_2NH_2$) **32a** and alcohol (R = CH_2CH_2OH) **34a**, and to their N-methylated analogues **32b** and **34b**, whose synthesis is reported in Scheme 5.

Briefly, compounds **7a** or **7b** were homologated to elongated amines **32a**,**b** via mesylation (MsCl, TEA) and cyanide displacement (nBu_4NCN, DMF) to give *N*-Boc nitriles **29a**,**b**, hydrogenation (H_2, Ni-Raney) to give *N*-Boc amines **30a**,**b** and *N*-Boc deprotection (HCl, MeOH; overall unoptimized yield: 25%, **32a** and 41%, **32b**). *N*-Boc deprotection of **29a** (HCl, MeOH) yielded also pure nitrile **31a** in quantitative yield (deprotection of **29b** was not attempted). *N*-Boc amines **30a**,**b** were converted to primary alcohols **34a**,**b** via nitrosation ($NaNO_2$, citric acid) and *N*-Boc deprotection (HCl, MeOH), although with poor yields (overall unoptimized yield: 12%, **34a** and 9%, **34b**).

Compounds **30a**,**b** were also used to access the 1-aza-2-oxobicyclo[5.3.0]decane amides **36a**,**b** (overall unoptimized yield: 50%, **36a** and 55%, **36b**), ureas **38a**,**b** (overall unoptimized yield: 31%, **38a** and 89%, **38b**), ethylamines **40a**,**b** (overall unoptimized yield: 24%, **40a** and 21%, **40b**) and benzylamines **40c**,**d** (overall unoptimized yield: 41%, **40c** and 48%, **40d**) (Scheme 6). Reaction conditions were similar to the ones used for the synthesis of secondary amines, amides and ureas in Schemes 3 and 4. Most compounds needed a final preparative HPLC purification to be obtained as pure materials.

Compound **32a** was then fully characterized with our structure-based, biophysical engine.

As to crystallography, we have recently obtained co-crystals of **32a** with the BIR3 domain of XIAP.[37] The XIAP BIR3/**32a** crystal structure reported in Figure 8 (superimposition between crystals' data and docking models of **32a** in XIAP BIR3 active site) is in

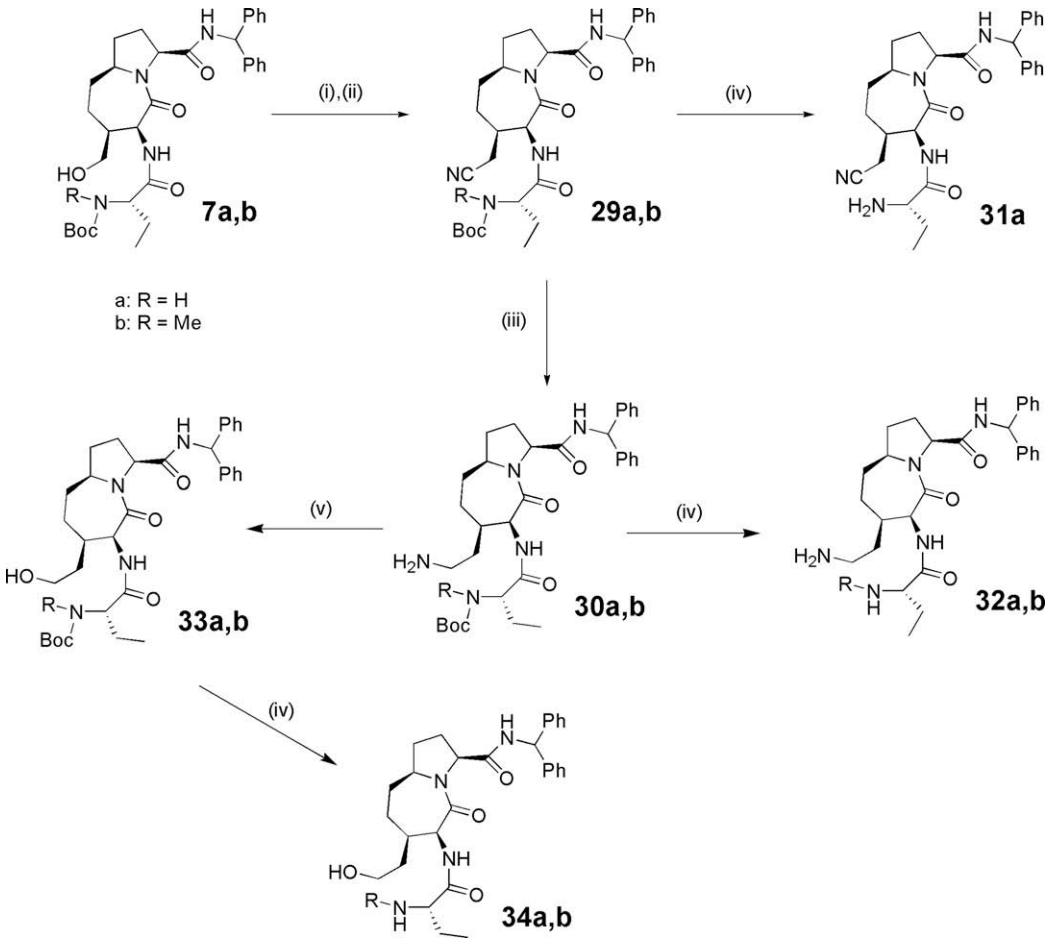

Scheme 5. Reagents and conditions: (i) MsCl, TEA, CH_2Cl_2, rt; (ii) nBu$_4$NCN, DMF, 80 °C; (iii) H_2, Ni-Raney; (iv) 3 N HCl in MeOH, rt; (v) $NaNO_2$, citric acid, THF, 0 °C to rt.

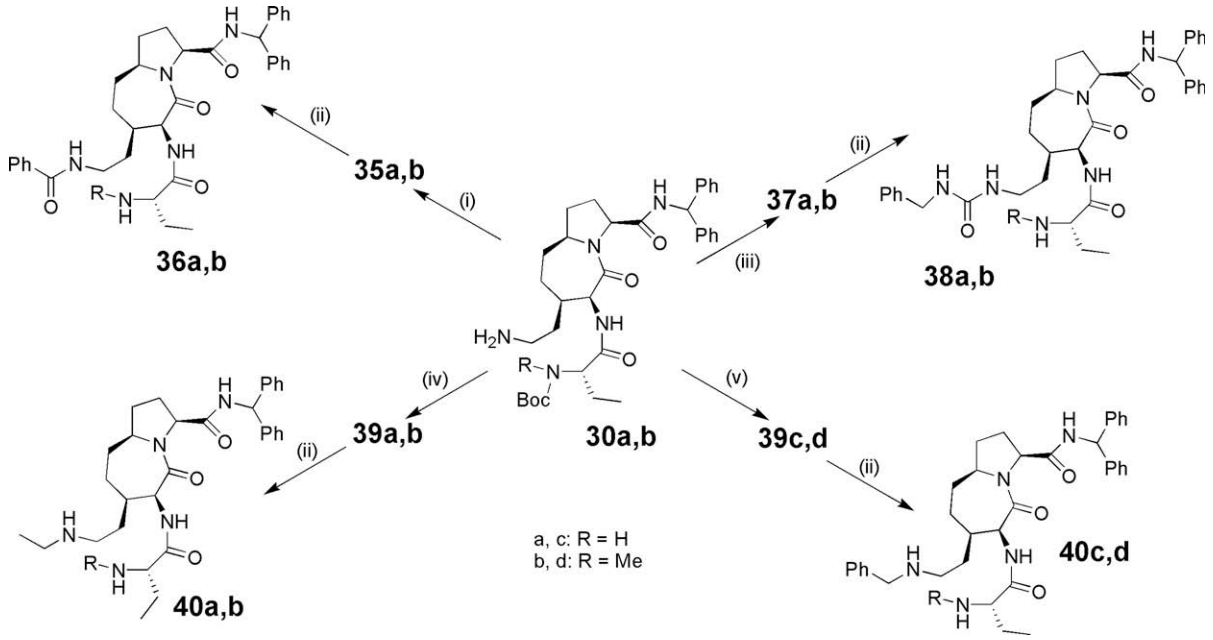

Scheme 6. Reagents and conditions: (i) PhCOCl, DIPEA, CH_2Cl_2, rt; (ii) 3 N HCl in MeOH, rt; (iii) $PhCH_2NCO$, DIPEA, CH_2Cl_2, rt; (iv) EtCHO, $NaBH(OAc)_3$, CH_2Cl_2, rt; (v) PhCHO, $NaBH(OAc)_3$, CH_2Cl_2, rt.

agreement with our predictions. The interactions between the 4-$CH_2CH_2NH_2$ arm and Asp309, and the prevention of ligand molecule shift observed for **4a** confirm the validity of the design criteria adopted.

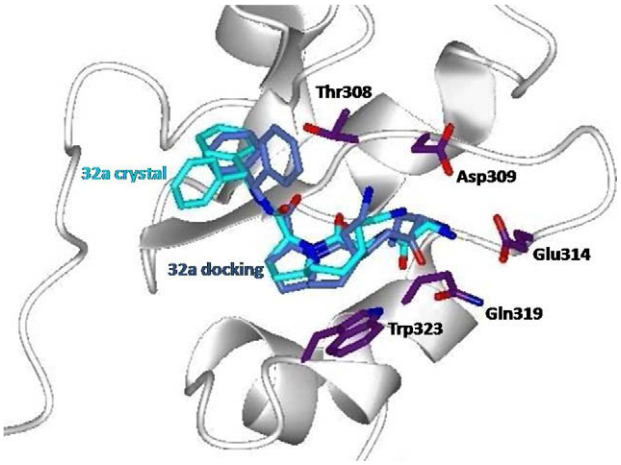

Figure 8. X-ray crystal structure of **32a** and XIAP BIR3. Superposition of the lowest free energy XIAP BIR3/**32a** docked model (**32a** light blue, protein light grey) on the XIAP BIR3/**32a** crystal structure (**32a** cyan, protein grey). Residues involved in the main stabilizing interactions are shown.

As to NMR, the STD–NMR spectra of **32a** (Fig. 9) in presence of various binding partners confirms different binding interactions of 4-substituted 1-aza-2-oxobicyclo[5.3.0]decanes with BIR2 and BIR3 domains. As seen for **3a** (Fig. 4), the diphenylamido and the ethylglycine moiety interact with BIR3 (lane A, 7.3 ppm-Ar amide, 6.0 ppm-H_{18}, 0.9 ppm-H_{15}, Fig. 9), while the construct linker-BIR2–BIR3 shows a putative linker-BIR2 interaction with the 4-substituted 1-aza-2-oxobicyclo[5.3.0]decane scaffold itself (lane B, 4.0 ppm-H_7, Fig. 9), although less intense than observed for **3a**. Interestingly, although the 4-$CH_2CH_2NH_2$ moiety ($H_{11} \approx 1.8$ ppm, $H_{19} \approx 2.9$ ppm) in **32a** does not interact with any of the targets, as seen previously for **4a** and **16a**, the interaction between its ethylglycine moiety and BIR3 (weak for **4a**, absent for **16a**) is restored at a comparable level with **3a**. This indicates, once again in accordance with crystallographic evidence, the non-shifted, **3a**-like binding mode of elongated **32a** with BIR3.

2.5. In vitro biology profiling

Reference compounds **1a**[30] and **1b**,[31] non-elongated compounds **3a–31a** (see Fig. 10) and elongated compounds **32a**–**40d** (see Fig. 11) were tested for their in vitro binding to XIAP BIR3 and linker-BIR2–BIR3 domains, using two reported assay formats.[39,40]

Their IC_{50} values on both fragments of full length XIAP are reported in Table 1. We derive for standard compound **1a** a $K_i = 200$ nM, definitely higher than the reported 25 nM value.[30] As to **1b**, we obtain a $K_i = 230$ nM versus the reported 61 nM value.[31] These discrepancies may stem from different environmental parameters and from K_i calculation methods, as discussed in details elsewhere.[36]

The data show how the introduction of a 4-substitution with N- or O-containing functional groups on the 1-aza-2-oxobicyclo[5.3.0]decane scaffold is often beneficial in terms of affinity for BIR3. For example, 4-CH_2X-subst. compounds bearing hydroxyl groups (**3a**), secondary amines (i.e., **18a** and **18b**), amides (i.e., **22c**) and ureas/thioureas (i.e., **26a** and **26b**) show around a twofold increase in potency, when compared to **1a** and **1b**. Interestingly, aromatic lipophilic extensions on the 4-arm, as in benzyl amine **18b**, benzamide **22c** and benzyl urea **26b**, were recommended by modelling studies. Furthermore, it is significant to observe that the 4-CH_2NH_2 substituted **4a** shows a reduced affinity for BIR3 ($IC_{50} \cong 1$ μM), while its 4-elongated homologue **32a** is more potent ($IC_{50} = 250$ nM). These results substantiate the crystallographic prediction of loss of potency for **4a** (overall shift towards the Asp309 residue, with concomitant loss of hydrogen bonds and hydrophobic interactions) and of increased potency for **32a** (optimization of the interaction between 4-CH_2NH_2 and Asp309,

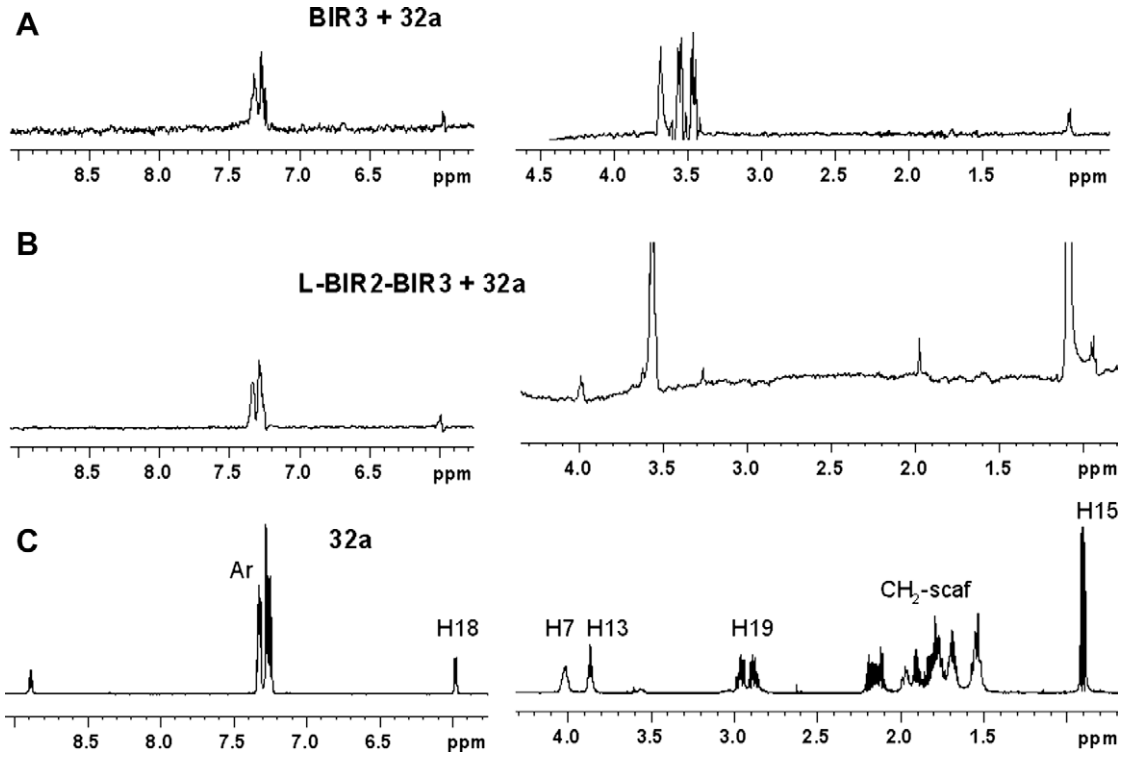

Figure 9. STD-NMR spectra of compound **32a** with BIR3 (A), linker BIR2–BIR3 (B) and as such (C).

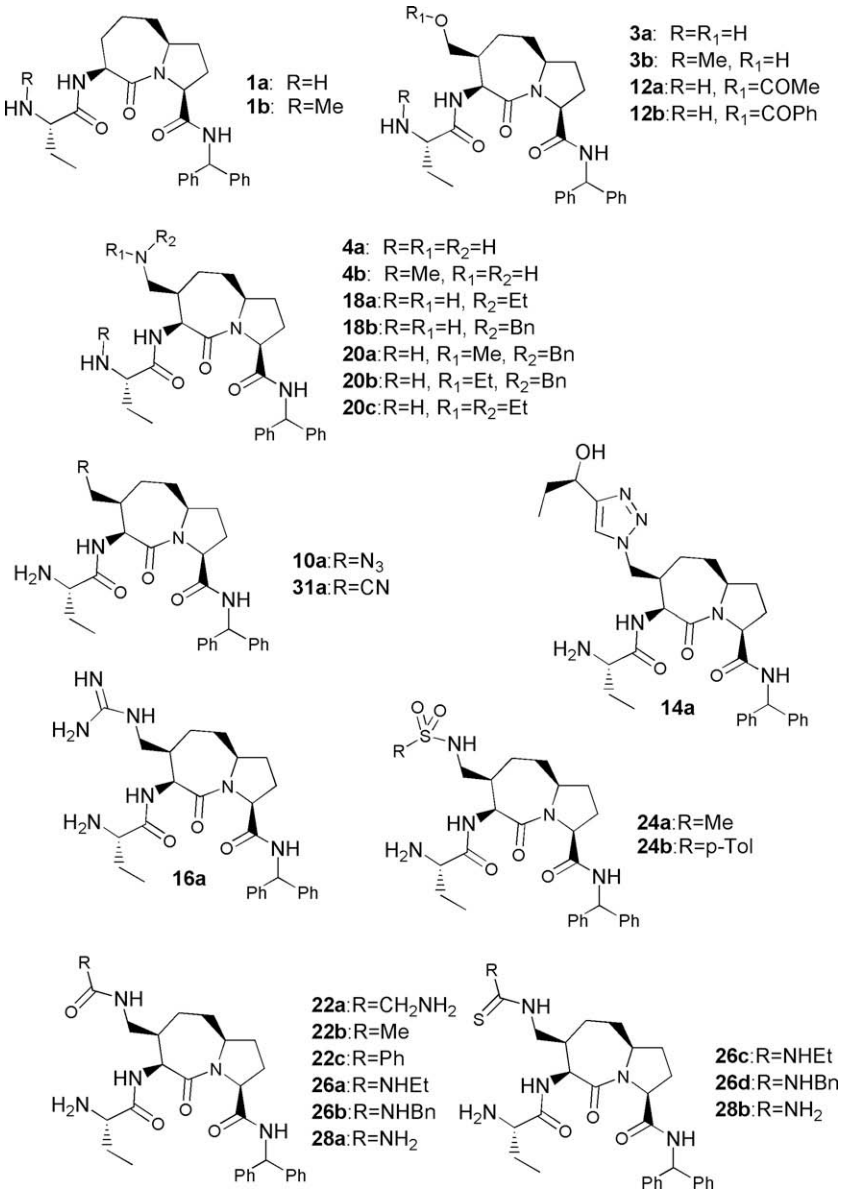

Figure 10. Chemical structures of 4-unsubstituted and non-elongated compounds **1a**–**31a**.

without binding-detrimental overall shifts). The same trend is observed on 4 N-substituted, non-elongated/elongated couples (**18a**/**40a**, **18b**/**40c**, **22c**/**36a**, **26b**/**38a**), where the increase in potency with elongation varies between 2 (**18a**/**40a**, **22c**/**36a**, **26b**/**38a**) and 6 (**18b**/**40c**).

This trend is not observed with non-elongated (**3a**) and elongated (**34a**) alcohols, which show similar potencies. This is once again in accordance with our structural data, which show no overall binding-detrimental shift in the active site pocket of BIR3 for **3a**. N-methylation on the ethylglycine residue in 4-unsubstituted, 1-aza-2-oxobicyclo[5.3.0]alkane-based Smac mimics only marginally decreases their affinity for the BIR3 domain of XIAP, while being beneficial in terms of cytotoxicity on cancer cells.[31] Comparing IC_{50} data on BIR3 for 8 NH/N-Me couples presented in this work (**3a**/**b**, **4a**/**b**, **32a**/**b**, **34a**/**b**, **36a**/**b**, **38a**/**b**, **40a**/**b**, **40c**/**d**), we confirm that N-methylated Smac mimics are potent BIR3 binders. Surprisingly, they are consistently better than their NH analogues, up to one order of magnitude (**4a**/**b**; in this case, N-methylation could influence the overall binding-detrimental shift in the active site pocket of BIR3 observed for **4a**), with the single exception of the **40c**/**d** couple.

Our results on the XIAP linker-BIR2–BIR3 construct are even more surprising. It has been shown[41,42] that dimeric Smac mimetics based on scaffold **2** have a low nanomolar-high picomolar IC_{50} on the bivalent binding construct, most likely due to their intramolecular binding to both BIR domains of the same biological target molecule.[43] Reference monomers **1a** and **1b** show similar IC_{50} values (around 4–500 nM) for both BIR3 and linker-BIR2–BIR3 constructs from XIAP. This is to be expected, as BIR3 is the high affinity binding site (K_d around 500 nM) for the Smac N-terminal AVPI peptide, while BIR2 is the lower affinity binding site (K_d around 10 μM) for the same peptide. Thus, adding the BIR2 domain to the XIAP binding construct should not change the measured K_d or IC_{50} for a monomer, while simultaneous binding to BIR2 and BIR3 by a dimeric molecule causes a significant increase in potency and mimicks the biological mode of action and potency of full length Smac. An indirect confirmation of this hypothesis is given by the similar potency of monomeric and dimeric Smac mimetics on the XIAP BIR3 single domain.[41,43] Most of our compounds show a significant increase in potency when tested on the linker-BIR2–BIR3 construct. For example, compounds **4a**, **16a**, **18b**, **20b**, **20c**, **26c**, **26d** and **28b** show a ≥4-fold increase in potency; and most

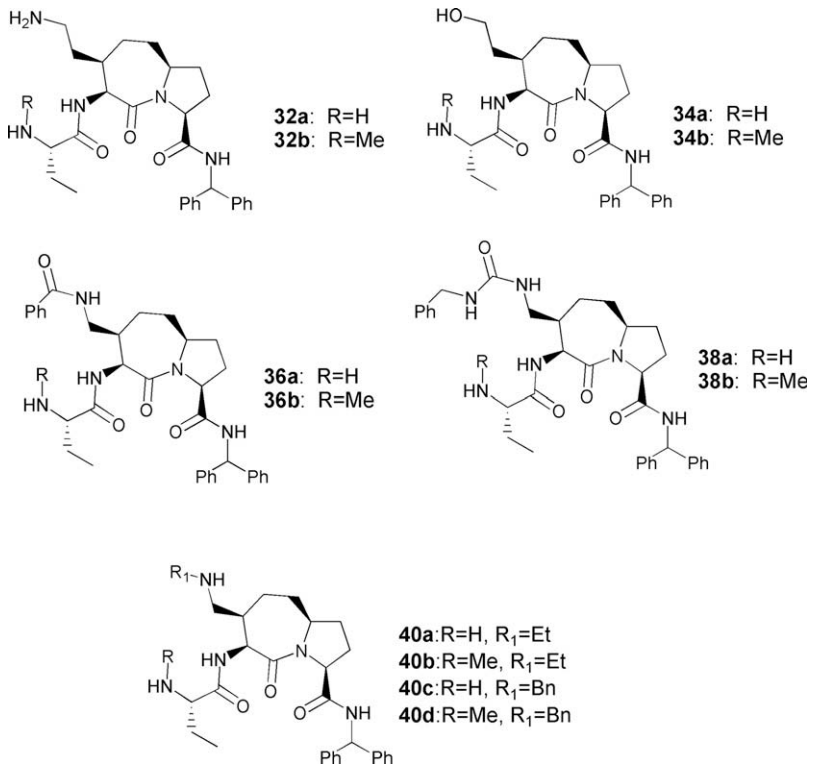

Figure 11. Chemical structures of elongated compounds **32a**–**40d**.

of other 4-substituted, N-containing functional groups show at least a twofold increase. Interestingly, most compounds containing an O-functional group on the 4-arm (i.e., **3a**, **3b**, **12a** and **34b**) show a much smaller potency increase. Although further experiments are needed to fully evaluate the extent and the relevance of this observation, we could now hypothesize that the different behaviour observed in STD–NMR studies by our Smac mimics, rather than pointing towards a reduction in affinity for the primary BIR3 binding site, indicates a gain of interactions with the secondary/linker-BIR2 binding site, leading to an overall increase in affinity for the linker-BIR2–BIR3 construct and, hopefully, for XIAP in cells and in animal models.

A smaller set of potent compounds was tested on a panel of tumour cell lines including MDA-MB-231 cells (breast), HL-60 cells (leukemia) and PC-3 cells (prostate). Their IC_{50} are reported in Table 2.

N-Methylation of the ethylglycine residue, as expected, gives beneficial effects on cytotoxicity, although not as much as observed for the 4-unsubstituted standard couple **1a**/**b** (≈1000 increase) on MDA-MB-231 cells.[31] The 8 NH/N-Me couples characterized here span from a 4–5-fold increase (**3a**/**b**) to a >10-fold increase (**4a**/**b**) on MDA-MB-231 cells. More resistant cell lines provide comparable cytotox results for the standard couple **1a**/**b** and for our compounds, never surpassing a twofold increase (**1a**/**b** and **4a**/**b**, PC-3; **36a**/**b** and **38a**/**b**, HL-60). A comparison between elongated (4-CH_2CH_2X, **E**) and non-elongated (4-CH_2X, **NE**) compounds provides unexpected results. Elongation causes a slight but consistent reduction in cytotoxicity in almost all **NE**/**E** couples (**3a**/**34a**, **3b**/**34b**, **4a**/**32a**, **4b**/**32b**, **18a**/**40a**, **18b**/**40c**, **22c**/**36a**, **26b**/**38a**), reaching a 4-fold maximum for **4b**/**32b** on MDA-MB-231 cells. An opposite trend was expected, due to affinity-driven (no **4a**-like shift in the active site) and lipophilic (one CH_2 more) contributions.

Cytotoxicity depends on the nature and the lipophilicity of 4-substituents. The ratio between the IC_{50} (potency in cells, **PC**) and the IC_{50} on linker-BIR2–BIR3 (linker-BIR2–BIR3 potency, **LBBP**) is reported for each compound tested on MBA-MB-231 cells in Table 3. A large PC/LBBP value indicates a potent compound with poor potency in cells, most likely due to limited access to its intracellular target/poor cell penetration; a value close to 1 indicates a potent compound both in cell-free and cellular assays.

The largest PC/LBBP ratio appears for reference compound **1a**, confirming its reported poor bioavailability in cells. This ratio is decreased ≈1000 times, without increasing LBBP, just by methylating its amino group as in **1b**.[31] Unfavourable PC/LBBP ratios are measured for 4-substituted compounds bearing small charged groups, that is, NH_2 (**4a** = 54.8; **32a** = 150; **4b** = 10; **32b** = 27.1). As already mentioned, beneficial effects are provided by N-methylation. Unexpectedly, a ≈3-fold increase of PC/LBBP ratio in elongated, more lipophilic compounds (**4a** vs **32a**, **4b** vs **32b**) was also observed. Favourable PC/LBBP ratios are obtained by replacing the charged NH_2 with polar, non-charged OH (**3a** = 3.55; **3b** = 1.18; **34b** = 1.73). A PC/LBBP decrease is also observed by functionalization of primary amines in 4, either as a non-charged amide (**22c** = 3.86) and as charged secondary amines (**18a** = 3.11; **18b** = 1.38). N-Methylation (positive effect, **3b** vs **3a**, **34b** vs **34a**, **36b** vs **36a**, **40b** vs **40a**, **40d** vs **40c**) and elongation (negative effect, **3a** vs **34a**, **3b** vs **34b**, **18a** vs **40a**, **18b** vs **40c**, **22c** vs **36a**) influence the ratio as seen for primary amines **4a**,**b** and **32a**,**b**. Benzyl ureas (**26b** = 35.1, **38a** = 144, **38b** = 20) show a surprisingly high PC/LBBP value, which cannot be explained by LBBP-related factors, as the compounds bind potently both BIR3 and linker-BIR2–BIR3. In particular, N-alkylation on position 4 elicits similar beneficial effects on cytotoxicity/cell penetration as N-methylation on the ethylglycine moiety (4-CH_2NH_2 **4a** = 54.8 vs 4-CH_2NHEt **18a** = 3.11 vs 4-CH_2NHCH_2Ph **18b** = 1.38), and the two effects are additive (4-$CH_2CH_2NH_2$ **32a** = 150 vs N-Me,4-$CH_2CH_2NH_2$ **32b** = 27.1 and 4-$CH_2CH_2NHCH_2Ph$ **40c** = 11.4, vs N-Me,4-$CH_2CH_2NHCH_2Ph$ **40d** = 5.2); is more favourable for activity than N-acylation (**18b**-benzyl amine vs **22c**-benzamide: slightly better cell-free potency,

Table 1
Experimentally determined IC_{50} of compounds **1a**, **1b**, **3a**–**40d** (fluorescence polarization-based assays) on XIAP BIR3 and ligand-BIR2–BIR3

Compound	IC_{50} BIR3[a,b]	RSD (%)	IC_{50} linker-BIR2–BIR3[a,b]	RSD (%)
1a	460 (K_i = 25)[c]	7	360	42
1b	530 (K_i = 61)[d]	11	420	31
3a	270	7	290	31
3b	230	12	200	21
4a	970	5	110	21
4b	100	14	54	48
10a	450	15	240	25
12a	400	8	320	59
12b	600	26	150	27
14a	370	8	220	23
16a	4400	54	390	30
18a	240	10	92	16
18b	320	4	72	20
20a	650	4	150	22
20b	440	12	110	21
20c	370	4	110	25
22a	430	11	150	25
22b	330	18	190	27
22c	260	12	110	30
24a	360	11	240	29
24b	510	81	160	31
26a	300	12	190	30
26b	240	9	97	22
26c	330	3	83	16
26d	380	6	54	18
28a	340	1	240	24
28b	220	14	54	21
31a	320	6	240	26
32a	250	2	86	31
32b	140	7	85	22
34a	280	11	70	33
34b	130	17	100	36
36a	120	16	58	23
36b	120	16	55	26
38a	140	15	75	31
38b	100	14	60	29
40a	110	9	56	30
40b	86	16	70	38
40c	49	12	35	31
40d	110	24	27	53

[a] Nanomolar values, see Section 4 for details.
[b] Average value from four measurements.
[c] K_i in brackets from Ref. 30.
[d] K_i in brackets from Ref. 31.

Table 2
Experimentally determined IC_{50} (μM) of compounds **1a**, **1b** and **3a**–**40d** on tumour cell lines

Compound	MDA-MB-231[a,b]	HL-60[a,b]	PC-3[a,b]
1a	>100(>10)[c]	24.5 ± 1.3	>100
1b	0.146 ± 0.007(0.1)[d]	20.2 ± 1.5	56.9 ± 1.1
3a	1.03 ± 0.68	6.5 ± 2.4	>100
3b	0.237 ± 0.003/	26.1 ± 1.8	>100
4a	6.03 ± 1.54	69.3 ± 3.55	>100
4b	0.542 ± 0.002	51.8 ± 0.06	51.7 ± 1.1
18a	0.286 ± 0.007	84.0 ± 4.0	>100
18b	0.099 ± 0.003	13.1 ± 2.2	24.1 ± 1.8
22c	0.425 ± 0.012	36.0 ± 7.0	80.1 ± 0.5
26b	3.4 ± 0.7	51.0 ± 0.01	>100
32a	12.9 ± 0.3	25.0 ± 1.8	85.2 ± 1.3
32b	2.3 ± 1.2	31.0 ± 1.3	>100
34a	1.8 ± 0.03	>100	>100
34b	0.173 ± 0.002	74.8 ± 5.3	>100
36a	0.93 ± 0.02	50.7 ± 0.2	>100
36b	0.21 ± 0.01	32.6 ± 5.0	>100
38a	10.8 ± 0.1	83.3 ± 9.6	>100
38b	1.2 ± 0.01	52.2 ± 0.1	83.5 ± 6.2
40a	8.0 ± 0.9	62.8 ± 0.2	>100
40b	1.3 ± 0.1	76.4 ± 11.3	>100
40c	0.4 ± 0.007	15.4 ± 8.6	39.2 ± 9.8
40d	0.141 ± 0.001	5.2 ± 0.2	7.8 ± 0.3

[a] IC_{50}, see Section 4 for details.
[b] Average value from 2 experiments, each point done in triplicate.
[c] Value in brackets from Ref. 30.
[d] Value in brackets from Ref. 31.

better PC/LBBP ratio); and favours bulky, lipophilic vs small alkyl groups (**18b**-benzyl amine vs **18a**-ethyl amine: slightly better cell-free potency, better PC/LBBP ratio).

The cytotoxic activity of 1-aza-2-oxobicyclo[5.3.0]alkane-based Smac mimics on HL-60 and PC-3 cells is much lower, as mirrored by higher PC1/LBBP (HL-60) and PC2/LBBP (PC-3) ratios, reported in Table 4.

Best ratios are obtained for HL-60 cells with alcohol **3a** (PC1/LBBP = 22.4) and for PC-3 cells with benzyl amine **40d** (PC2/LBBP = 288.9), and in general with 4-unsubstituted standard **1b** (PC1/LBBP = 48.1 and PC2/LBBP = 135.5). Most trends observed for MDA-MB-231 cells are also applicable here (**18b** better than **18a** and **22c**; elongated compounds slightly worse than their non-elongated counterparts), while others are not (N-alkylation on ethylglycine either neutral or negative for cytotoxicity, see for example **3a** vs **3b**, **32a** vs **32b**). It remains to be seen if the moderate activity of our Smac mimics on HL-60 and PC-3 cells, probably due to a mix of target-related and permeability-related factors, can be improved.

We have shown how 4-substitution on 1-aza-2-oxobicyclo[5.3.0]decanes is suitable to modulate their potency and physico-chemical properties (i.e., lipophilicity and solubility). As to the latter, some promising compounds were submitted to a preliminary early ADMET assay panel, including solubility, metabolic stability and permeability, so to determine their appropriateness as cell-permeable, metabolically stable and soluble leads (Table 5).

Some interesting observations can be made, despite the small number of assays and the limited set of tested compounds. In terms of metabolic stability (human CYP3A4), most compounds are reasonably stable, with some warnings for 4-N elongated amides **36a**,**b** and ureas **38a**,**b**. Alcohols, primary and secondary amines are at least as stable as 4-unsubstituted standards **1a**,**b**. In terms of solubility (acidic and neutral pH), both N-methylation of the ethylglycine residue and introduction of 4-N or 4-O contain-

Table 3
Experimentally determined ratios between IC_{50} on linker-BIR2–BIR3 (LBBP) and IC_{80} on MDA-MB-231 cells (PC) for compounds **1a**, **1b** and **3a**–**40d**

Compound	CFP[a]	PC[b]	PC/LBBP
1a	360	>100	>280
1b	420	0.146	.348
3a	290	1.03	3.55
3b	200	0.237	1.18
4a	110	6.03	54.8
4b	54	0.542	10.0
18a	92	0.286	3.11
18b	72	0.099	1.38
22c	110	0.425	3.86
26b	97	3.4	35.1
32a	86	12.9	150
32b	85	2.3	27.1
34a	70	1.8	25.7
34b	100	0.173	1.73
36a	58	0.93	16.0
36b	55	0.21	3.82
38a	75	10.8	144
38b	60	1.2	20
40a	56	8.0	142.9
40b	70	1.3	18.6
40c	35	0.4	11.4
40d	27	0.141	5.2

[a] Nanomolar values, see Table 1 and Section 4 for details.
[b] Micromolar values, see Table 2 and Section 4 for details.

Table 4
Experimentally determined ratios between IC_{50} on linker-BIR2–BIR3 (LBBP) and IC_{80} on HL60 (PC1) and PC-3 cells (PC2) for compounds **1b** and **3a**–**40d**

Compound	CFP[a]	PC1/PC2[b]	PC1,2/LBBP[c]
1b	420	20.2/56.9	48.1/135.5
3a	290	6.5/ND[d]	22.4/ND
3b	200	26.1/ND	130.5/ND
4a	110	69.3/ND	630ND
4b	100	51.8/51.7	518/517
18a	92	84.0/ND	913.0/ND
18b	72	13.1/24.1	181.9/334.7
22c	110	36.0/80.1	327.3/728.2
26b	97	51.0/ND	525.6/ND
32a	86	25.0/85.2	290.7/990.7
32b	85	31.0/ND	364.7/ND
34b	100	74.8/ND	748/ND
36a	58	50.7/ND	874.1/ND
36b	55	32.6/ND	592.7/ND
38a	75	83.3/ND	1110.7/ND
38b	60	52.2/83.5	870/1391.7
40a	56	62.8/>100	1121.4/ND
40b	70	76.4/ND	1091.4/ND
40c	35	15.4/39.2	440/1120
40d	27	5.2/7.8	192.6/288.9

[a] Nanomolar values, see Table 1 and Section 4 for details.
[b] Micromolar values, see Table 2 and Section 4 for details.
[c] First value PC1/LBBP, second value PC2/LBBP.
[d] ND, not detectable.

Table 5
Early ADMET characterization of compounds **1a**, **1b** and **3a**–**40d** on a preliminary eADME panel

Compound	Metab. Stab.[a]	Solubility[b]	PAMPA[a,c]
1a	87	19/23	23
1b	83	248/175	42
3a	79	111/183	17
3b	86	210/172	30
4a	93	138/168	2
4b	78	233/>250	<1
18a	81	159/182	<1
22c	81	81/134	21
26b	73	36/21	4
32a	75	169/207	<1
32b	86	>250/207	<1
36a	65	185/244	4.1
36b	43	179/243	3
38a	65	145/216	<1
38b	51	148/194	<1
40b	90	184/191	<1
40d	81	>250/>250	4.3

[a] Human CYP3A4, see Section 4 for more details.
[b] pH7.4/pH3, see Section 4 for details.
[c] Parallel Artificial Membrane Permeability Assay (PAMPA), see Section 4 for more details.

ing substituents is beneficial. Interestingly, **40d** shows an extremely high solubility profile at both tested pHs, and is a promising candidate for further biological profiling due to its balanced activity; conversely, ureas **26b** and (to a lower extent) **38a**,**b** have a lower solubility, which may partially justify their reduced cytotoxicity. In terms of cellular permeability (surrogate artificial membrane penetration, PAMPA), highest values are observed for 4-unsubstituted and 4-O substituted compounds. As to 4-N substitutions, only a few compounds (amides **22c**, **38a**,**b**, urea **26b** and benzylamine **40d**) have a measurable permeability. Rather than searching for a quantitative relationship, we may safely say that compounds with negligible passive permeability (<1, Table 5) have PC/LBBP ratios $\geq$10.0, that is, do not show cellular activities comparable with their cell-free potencies; weakly cytotoxic ureas **38a**,**b** (PC/LBBP = 144 and 20, respectively) are a typical example.

3. Conclusion

In this paper we report the synthesis of several 4-substituted 1-aza-2-oxobicyclo[5.3.0]decanes as monomeric Smac mimics, introducing small and large, charged and neutral N- and O-substitutions on non-elongated and elongated 4-side chains (respectively 1 and 2 carbon atoms between the scaffold and the heteroatom). The compounds were rationally designed using theoretical and experimental data obtained through computational methods, NMR and crystallography techniques. Structural theories derived from these data, presented and discussed here, rationalize the binding mode of the compounds, account for most of significant target binding differences, and will be used to further optimize their properties in second generation analogues. The compounds were tested for inhibition of BIR3 and linker-BIR2–BIR3, two fragments of the protein XIAP, a popular and validated target in apoptosis/oncology. Several compounds exhibited low nanomolar activities on both targets, with best results obtained for compounds bearing a lipophilic N-substituent in position 4 (e.g., benzamides **36a**,**b**, benzyl ureas **38a**,**b**, secondary amines **40a–d**). Cytotoxicity of Smac mimics was measured on three tumour cell lines with varying sensitivity to XIAP-dependent apoptosis (MDA-MB-231, HL-60 and PC-3). The compounds exhibited nanomolar (MDA-MB-231)/micromolar (HL-60, PC-3) potencies, depending on their affinity for the target and on their drug-like properties. The relationship between cytotox (PC) and cell-free potency (LBBP) was elucidated also by means of a preliminary set of results on ADMET assays. We suppose that a compromise between in vitro potency, stability, good solubility and measurable permeability should produce drug-like, bioavailable compounds: for example, standard compound **1b**, 4-hydroxy compound **3b** and 4-benzylamine **40d** satisfy these criteria and are potent cytotoxic agents.

Although further optimization is ongoing, we believe that a compound such as **40d** (elongated N-Me,4-$CH_2CH_2NHCH_2Ph$), with low nanomolar potency on linker-BIR2–BIR3 and on MDA-MB-231 cells, and low micromolar potency on both HL-60 and PC-3 cells represents an early lead which will be further characterized in in vitro and in vivo relevant models. Interestingly, while submitting this paper we became aware of novel potent, monomeric Smac mimics[44] which contain some of the features present in our 'best' 4-substitutions, although being built on a different scaffold.

4. Experimental

4.1. Chemical procedures

4.1.1. General methods

^1H NMR spectra were recorded on Bruker Avance in $CDCl_3$, CD_3OD or D_2O as solvent at 400 or 600 MHz. ^{13}C NMR spectra were recorded in $CDCl_3$, CD_3OD or D_2O as solvent at 100 or 125 MHz. Coupling constants are given in hertz and are rounded to the nearest 0.1 Hz. Purifications were carried out either by flash chromatography on silica gel (particle size 60 μm, 230–400 mesh), Kieselgel, or by Biotage™ flash chromatography [Biotage columns Si-12-M (150 × 12 mm; silica gel (40–63 μm), flow rate 12 mL/min); Si-25-M (150 × 25 mm; silica gel (40–63 μm), flow rate 25 mL/min)], or by Biotage™ C_{18} reverse phase chromatography [Biotage column C_{18}HS (150 × 25 mm; KP-C_{18}-HS (35–70 μm), flow rate 25/mL/min)]. Final products were purified by C_{18} reverse phase semi-preparative HPLC using either a Waters X-Terra RP_{18} OBD column (19 mm × 10.0 cm, 5 μm) or a Supelco Ascentis C_{18} column (21.2 mm × 15.0 cm, 5 μm). Solvents were distilled and dried according to standard procedures, and reactions requiring anhydrous conditions were performed under nitrogen or argon. Solvents for the reactions were used directly from the bottle if

not specified. Optical rotations $[\alpha]_D^{20}$ were measured in cells of 1 dm pathlength and 1 mL capacity with a Perkin Elmer 241 polarimeter. LC–MS data were collected with an Agilent 1100 HPLC connected to a Bruker Esquire 3000+ ion trap mass spectrometer through an ES interface.

4.1.2. General procedure A—synthesis of compounds 6

Compound **5** (2.05 g, 5.3 mmol) was dissolved in 26.5 mL of a 3 N methanolic HCl solution. The resulting mixture was stirred at room temperature for 48 h and then condensed under reduced pressure. The crude product was redissolved in CH_2Cl_2 and washed once with a saturated solution of $NaHCO_3$. The organic layer was dried over Na_2SO_4, filtered and the solvent was removed under reduced pressure. The crude methyl ester was purified by Biotage™ C_{18} reverse phase chromatography. Biotage™ eluant conditions: from 90 H_2O and 10% CH_3CN to 100% CH_3CN. Yield 90% (1.65 g, MW 344.17, 4.79 mmol) of pure methyl ester as an amorphous white solid. *Analytical characterization*: $[\alpha]_D^{20} = -142.0$ (*c* 1.15, MeOH); ^{1}H NMR (400 MHz, $CDCl_3$): δ: 7.44 (d, *J* = 6.8 Hz, 2H), 7.35–7.23 (m, 3H), 4.74 (dd, *J* = 7.2, 4.4 Hz, 1H), 4.46 (d, *J* = 13.6 Hz, 1H), 4.13 (dd, *J* = 9.2, 7.6 Hz, 1H), 3.87 (m, 1H), 3.74, (s, 3H), 3.65 (d, *J* = 13.6 Hz, 1H), 3.52 (dd, *J* = 7.6, 6.0 Hz, 1H), 3.18 (d, *J* = 10.0 Hz, 1H), 2.78 (m, 1H), 2.30 (m, 1H), 2.14–2.01 (m, 3H), 1.95–1.63 (m, 4H); ^{13}C NMR (100 MHz, $CDCl_3$): δ: 172.6, 168.8, 137.4, 129.0, 128.2, 127.2, 73.2, 71.4, 61.4, 59.9, 58.8, 52.4, 44.9, 33.9, 33.3, 32.2, 27.4; ESI-MS: *m*/*z* 344.9 $[M+H]^+$, 711.0 $[2M+Na]^+$.

Simultaneous N–O hydrogenolytic cleavage and benzyl deprotection was performed using the H-Cube™ continuous-flow hydrogenation reactor. The methyl ester (1.65 g, 4.79 mmol) was dissolved in 85:15 EtOH/water (190 mL, ≈0.025 M final concentration) and reduced over 10% Pd/C catalyst (hydrogen pressure: 10 bar, *T* = 85 °C, flow: 0.7 mL/min). The reaction was monitored by LC–MS. After reaction completion the solvent was evaporated under reduced pressure. The crude aminoalcohol was obtained in quantitative yield and used without any further purification. ESI-MS: *m*/*z* 256.8 $[M+H]^+$.

Dry DIPEA (2 equiv) was added to a solution of *N*-Boc protected aminoacid (1.2 equiv), EDC·HCl (1.2 equiv) and HOBt (1.2 equiv) in dry CH_2Cl_2 at room temperature and under a nitrogen atmosphere. The solution was stirred for 10 min before adding a solution of the aminoalcohol (1 equiv) in CH_2Cl_2 (final concentration of aminoalcohol: 0.1 M). The reaction mixture was stirred at room and monitored by LC–MS. After 1 h, the solution was diluted with CH_2Cl_2 and then washed once with 5% citric acid and saturated $NaHCO_3$. The organic layer was dried over Na_2SO_4 and evaporated under reduced pressure. The crude product was purified by Biotage™ C_{18} reverse phase chromatography.

4.1.2.1. Compound 6a. Compound **6a** was synthesized by general procedure A, starting from compound **5** (2.05 g, 5.3 mmol). Biotage™ eluant conditions: from 90 H_2O and 10% CH_3CN to 100% CH_3CN. Yield 70% (1.48 g, MW 441.52, 3.35 mmol) of pure **6a** as an amorphous white solid. *Analytical characterization*: $[\alpha]_D^{20} = -146.5$ (*c* 0.71, MeOH); ^{1}H NMR (400 MHz, $CDCl_3$): δ: 7.53 (d, *J* = 3.5 Hz, 1H), 5.07 (d, *J* = 7.6 Hz, 1H), 4.56 (dd, *J* = 8.5, 4.0 Hz, 1H), 4.48 (dd, *J* = 10.0 Hz, 7.5, 1H), 4.03 (m, 1H), 3.89 (m, 1H), 3.73 (s, 3H), 3.66 (m, 1H), 3.31 (dd, *J* = 12.0, 3.0 Hz, 1H), 2.30–2.23 (m, 1H), 2.15–1.97 (m, 4H), 1.90–1.75 (m, 4H), 1.69–1.58 (m, 2H), 1.43 (s, 9H), 0.95 (t, *J* = 7.5 Hz, 3H); ^{13}C NMR (100 MHz, $CDCl_3$): δ: 173.9, 172.4, 170.2, 155.6, 80.2, 64.3, 60.6, 58.8, 56.6, 54.1, 52.3, 41.5, 32.8, 31.2, 28.2, 25.7, 10.1. ESI-MS: *m*/*z* 441.9 $[M+H]^+$, 463.9 $[M+Na]^+$.

Full analytical characterization of compound **6b** is reported in the Supplementary data.

4.1.3. General procedure B—synthesis of compounds 7

A 2 N aqueous LiOH solution (7.0 equiv) was slowly added to an ice cooled, stirred solution of methyl ester **6** (1.0 equiv) in 1,4-dioxane (0.25 M concentration for **6**). The reaction mixture was then stirred at room temperature until complete hydrolysis of the starting material. The cloudy solution was concentrated after 3 h, the residue was taken up in CH_2Cl_2 and water, and acidified to pH 3 with aqueous 2 N HCl. The organic layer was dried over Na_2SO_4, and then the solvent was removed under reduced pressure. The crude carboxylic acid, obtained as amorphous white solids, did not require further purification.

4.1.3.1. Acid a. Quantitative yield (4.27 g, MW 427.49, 10.0 mmol), starting from methyl ester **6a** (4.41 g, 10.0 mmol). *Analytical characterization*: $[\alpha]_D^{20} = -123.0$ (*c* 0.61, MeOH); ^{1}H NMR (400 MHz, $CDCl_3$): δ: 7.76 (d, *J* = 6.5 Hz, 1H), 7.20 (br s, 1H), 5.33 (m, 1H), 4.56 (m, 2H), 4.09 (m, 1H), 3.91 (d, *J* = 7.5 Hz, 1H), 3.64 (d, *J* = 11.6 Hz, 1H), 3.43 (d, *J* = 9.5 Hz, 1H), 2.26 (d, *J* = 6.5 Hz, 1H), 2.12–1.62 (m, 10H), 1.42 (s, 9H), 0.95 (t, *J* = 6.5 Hz, 3H); ^{13}C NMR (100 MHz, $CDCl_3$): δ: 173.8, 173.5, 171.0, 156.0, 80.4, 64.3, 60.8, 60.4, 59.0, 56.5, 54.0, 41.2, 33.4, 32.9, 31.0, 28.2, 27.6, 25.7, 10.1. ESI-MS: *m*/*z* 427.9 $[M+H]^+$, 877.8 $[2M+Na]^+$.

Dry DIPEA (1.5 equiv) was added to a solution of carboxylic acid (1.0 equiv), EDC·HCl (1.2 equiv),and HOBt (1.2 equiv) in dry CH_2Cl_2. The solution was stirred for 10 min, then Ph_2CHNH_2 (1.2 equiv) and dry DIPEA (2 equiv) in dry CH_2Cl_2 (final concentration of the acid: 0.1 M) were added. The reaction mixture was stirred at room temperature for 1 h, then diluted with CH_2Cl_2 and washed once with 5% citric acid and saturated $NaHCO_3$. The organic layer was dried over Na_2SO_4 and evaporated under reduced pressure. The residues were purified by Biotage™ C_{18} reverse phase chromatography.

4.1.3.2. Compound 7a. Compound **7a** was synthesized by general procedure B, starting from acid **a** (4.27 g, 10.0 mmol). Biotage™ eluant conditions: from 90 H_2O and 10% CH_3CN to 100% CH_3CN. Yield 76% (4.5 g, MW 592.73, 7.6 mmol) of pure **7a** as an amorphous white solid. *Analytical characterization*: $[\alpha]_D^{20} = -125.0$ (*c* 1.48, MeOH); ^{1}H NMR (400 MHz, $CDCl_3$): δ: 7.97 (d, *J* = 8.4 Hz, 1H), 7.62 (d, *J* = 7.2 Hz, 1H), 7.35–7.15 (m, 10H), 6.21 (d, *J* = 8.8 Hz, 1H), 5.17 (d, *J* = 7.2 Hz, 1H), 4.73 (d, *J* = 7.6 Hz, 1H), 4.49 (m, 1H), 4.10 (m, 1H), 3.77 (dd, *J* = 17.6, 8.5 Hz, 1H), 3.67 (d, *J* = 10.8 Hz, 1H), 3.28 (dd, *J* = 12.0, 3.2 Hz, 1H), 2.38 (dd, *J* = 12.0, 6.8 Hz, 1H), 2.23 (m, 1H), 2.10–1.95 (m, 2H), 1.89–1.55 (m, 5H), 1.43 (s, 9H), 1.30–1.10 (m, 2H), 0.96 (t, 7.2 Hz, 3H); ^{13}C NMR (100 MHz, $CDCl_3$): δ: 173.9, 171.7, 171.1, 169.6, 155.8, 142.0, 141.2, 128.6, 128.4, 127.4, 127.2, 126.9, 80.3, 64.2, 61.2, 58.9, 56.8, 53.9, 41.5, 34.0, 33.2, 31.1, 28.3, 25.8, 25.6, 21.0, 14.2, 10.2. ESI-MS: *m*/*z* 593.1 $[M+H]^+$, 615.1 $[M+Na]^+$.

Full analytical characterization of **acid b** and of compound **7b** is reported in the Supplementary data.

4.1.4. General procedure C—synthesis of compounds 8

Dry TEA (4.0 equiv) and MsCl (4.0 equiv) were added to a stirred solution of alcohol **7** (1.0 equiv) in dry CH_2Cl_2 (0.25 M concentration for **7**) under argon atmosphere at 0 °C. The reaction mixture was stirred at room temperature overnight. After reaction completion, the resulting mixture was diluted with CH_2Cl_2 and washed once with saturated NH_4Cl. The organic layer was dried over Na_2SO_4, and then the solvent removed under reduced pressure. The crude product was dissolved in dry DMF (0.1 M concentration) under argon at room temperature, and then NaN_3 (10 equiv) was added. The reaction mixture was stirred at 80 °C overnight. After reaction completion, the mixture was filtered on a Celite pad after dilution with CH_2Cl_2. The solvent was then removed under reduced

pressure, and the crude product was purified by flash chromatography.

4.1.4.1. Compound 8a. Compound **8a** was synthesized by general procedure C, starting from alcohol **7a** (1.18 g, 2.0 mmol). Eluant mixture: petroleum ether/EtOAc 30:70. Yield 51% (635 mg, MW 617.74, 1.02 mmol) of pure **8a** as an amorphous white solid. *Analytical characterization*: $[\alpha]_D^{20} = -109.9$ (*c* 0.62, MeOH); ^{1}H NMR (400 MHz, $CDCl_3$): δ: 7.82 (d, *J* = 8.8 Hz, 1H), 7.30–7.13 (m, 10H), 7.21 (d, *J* = 6.4 Hz, 2H), 7.11 (d, *J* = 6.8 Hz, 1H), 6.14 (d, *J* = 8.8 Hz, 1H), 4.92 (br d, *J* = 7.2 Hz, 1H), 4.64 (d, *J* = 7.6 Hz, 1H), 4.50 (dd, *J* = 10.0 Hz, 8.0, 1H), 3.96 (dd, *J* = 13.6, 7.2 Hz, 1H), 3.76 (dd, *J* = 17.6, 9.2 Hz, 1H), 3.45 (dd, *J* = 12.4, 3.6 Hz, 1H), 3.06 (dd, *J* = 12.4, 9.2 Hz, 1H), 2.36 (dd, *J* = 12.4, 6.8 Hz, 1H), 2.18 (m, 1H), 1.95 (m, 1H), 1.82–1.44 (m, 6H), 1.39 (s, 9H), 1.30–1.1 (m, 2H), 0.89 (t, *J* = 7.2 Hz, 3H); ^{13}C NMR (100 MHz, $CDCl_3$): δ: 172.4, 171.3, 169.4, 155.8, 142.0, 141.1, 128.7, 128.6, 127.3, 127.2, 80.3, 61.0, 58.9, 56.8, 56.4, 53.6, 53.5, 40.0, 34.2, 33.3, 32.0, 28.3, 25.5, 21.0, 10.2. ESI-MS: *m*/*z* 618.1 $[M+H]^+$, 640.1 $[M+Na]^+$.

Full analytical characterization of compound **8b** is reported in the Supplementary data.

4.1.5. General procedure D—synthesis of compounds 9

A 1 N solution of $(CH_3)_3P$ in toluene (1.5 equiv) was added to a stirred solution of azide **8** (1.0 equiv) in dry CH_2Cl_2 (0.67 M concentration for **8**) under argon atmosphere at room temperature. After 2 h, an excess of 1 N aqueous HCl was added to the reaction mixture, which was stirred at room temperature for further 10–20 min. After reaction completion, the reaction mixture was extracted with CH_2Cl_2 (3 times), the organic layers were combined and dried over Na_2SO_4, and the solvent was removed under reduced pressure. The crude product was used without further purification.

4.1.5.1. Compound 9a. Compound **9a** was synthesized by general procedure D, starting from azide **8a** (617 mg, 1.0 mmol). Yield 92% (578 mg, MW 628.20, 0.92 mmol) of pure hydrochloride salt of **9a** as an amorphous white solid. *Analytical characterization*: $[\alpha]_D^{20} = -68.5$ (*c* 1.31, MeOH); ^{1}H NMR (400 MHz, $CDCl_3$): δ: 8.39 (br s, 3H), 8.04 (br s, *J* = 7.2 Hz, 1H), 7.82 (d, *J* = 8.4 Hz, 1H), 7.40–7.20 (m, 10H), 6.18 (d, *J* = 8.4 Hz, 1H), 5.12 (d, *J* = 6.4 Hz, 1H), 4.71 (d, *J* = 7.2 Hz, 1H), 4.49 (t, *J* = 8.0 Hz, 1H), 4.05 (q, *J* = 7.2 Hz, 1H); 3.74 (q, *J* = 8.4 Hz, 1H); 2.90 (br s, 2H); 2.40 (m, 1H), 2.21 (m, 1H), 2.05–1.55 (m, 7H), 1.47 (s, 9H), 1.33 (m, 1H), 1.22 (m, 1H), 0.99 (t, *J* = 7.6 Hz, 3H); ^{13}C NMR (100 MHz, $CDCl_3$): δ: 175.9, 170.1, 169.4, 142.2, 141.1, 128.7, 127.5, 127.4, 127.3, 80.3, 61.3, 58.7, 57.1, 53.8, 42.8, 38.1, 34.0, 33.3, 32.0, 29.0, 28.3, 25.8, 25.0, 10.4. ESI-MS: *m*/*z* 592.1 $[M+H]^+$, 614.1 $[M+Na]^+$.

Full analytical characterization of compound **9b** is reported in the Supplementary data.

4.1.6. General procedure E—synthesis of compounds 11

Pyridine (81 μL, 1.0 mmol), a carboxylic acid chloride RCOCl (0.10 mmol) and DMAP (12 mg, 0.02 mmol) were sequentially added to a stirred solution of **7a** (59 mg, 0.10 mmol) in dry CH_2Cl_2 (2 mL). The reaction mixture was stirred at room temperature overnight, the solvent was removed under reduced pressure and the crude product was purified by Biotage™.

4.1.6.1. Compound 11a. Compound **11a** was synthesized by general procedure E. Biotage™ eluant conditions: from 1% of MeOH and 99% of CH_2Cl_2 to 10% of MeOH and 90% of CH_2Cl_2. Yield 92% (58 mg, MW 634.74, 0.092 mmol) of pure **11a** as an amorphous white solid. *Analytical characterization*: $[\alpha]_D^{20} = -105.0$ (*c* 1.28, MeOH); ^{1}H NMR (400 MHz, $CDCl_3$): δ: 7.93 (d, *J* = 8.8 Hz, 1H), 7.38–7.19 (m, 10H), 7.10 (d, *J* = 8.4, 1H), 6.23 (d, *J* = 8.8 Hz, 1H), 5.01 (d, *J* = 6.8 Hz, 1H), 4.73 (d, *J* = 7.6, 1H), 4.67 (t, *J* = 8.4, 1H), 4.06 (m, 1H), 4.01 (m, 2H), 3.87 (dd, *J* = 17.6, 8.8 Hz, 1H), 2.44 (m, 1H), 2.26 (m, 1H), 2.06 (s, 3H), 1.88 (m, 4H), 1.80–1.60 (m, 3H), 1.55 (m, 1H), 1.47 (s, 9H), 1.22–1.10 (m, 1H), 0.97 (t, 7.6 Hz, 3H); ^{13}C NMR (100 MHz, $CDCl_3$): δ: 172.1, 171.7, 170.6, 169.5, 142.1, 141.2, 128.7, 128.6, 127.4, 127.3, 127.2, 65.4, 61.0, 58.7, 56.7, 56.3, 52.9, 39.1, 34.3, 33.4, 31.5, 28.3, 25.6, 20.9, 10.8. ESI-MS: *m*/*z* 635.0 $[M+H]^+$, 657.0 $[M+Na]^+$.

Full analytical characterization of compound **11b** is reported in the Supplementary data.

4.1.6.2. Synthesis of 13a. A 0.9 M water solution of sodium ascorbate (45 μL, 0.4 mmol) and a 0.3 M water solution of $Cu(OAc)_2$ (65 μL, 0.02 mmol) were sequentially added to stirred solutions of compound **8a** (62 mg, 0.10 mmol) and of 1-pentynyl-3-ol (8.6 μL, 0.10 mmol) in a 1:1 mixture of H_2O/^{t}BuOH (300 μL). The reaction mixture was stirred overnight at room temperature and then the solvent was removed under reduced pressure. The crude product was purified by Biotage™. Biotage™ eluant conditions: 1% of MeOH and 99% of CH_2Cl_2 to 10% of MeOH and 90% of CH_2Cl_2. Yield 58% (41 mg, MW 701.85, 0.058 mmol) of pure **13a** as an amorphous white solid. *Analytical characterization*: $[\alpha]_D^{20} = -50.0$ (*c* 0.88, $CHCl_3$); ^{1}H NMR (400 MHz, $CDCl_3$): 7.75 (dd, *J* = 8.4, 2.8 Hz, 1H), 7.35–7.00 (m, 11H), 6.11 (d, *J* = 8.4 Hz, 1H), 4.99 (d, *J* = 6.4 Hz, 1H), 4.76 (br s, 1H), 4.63 (m, 2H), 4.43 (m, 1H), 4.08 (m, 1H), 3.92 (m, 1H), 2.71 (m, 1H), 2.32 (m, 1H), 2.12 (m ,1H), 2.05 (m, 1H), 1.95–1.45 (m, 10H), 1.32 (s, 9H), 1.18 (s, 3H), 1.15–1.05 (m, 1H), 1.00–0.85 (m, 6H); ^{13}C NMR (100 MHz, $CDCl_3$): 172.9, 170.7, 169.3, 141.8, 141.3, 128.7, 127.5, 127.3, 127.1, 80.3, 68.4, 61.2, 58.8, 56.8, 56.3, 54.0, 52.2, 40.3, 33.8, 33.3, 31.7, 30.3, 29.7, 28.3, 25.7, 10.2, 9.8. ESI-MS: *m*/*z* 702.5 $[M+H]^+$, 724.5 $[M+Na]^+$.

4.1.6.3. Synthesis of 15a. *N*,*N*′-Bis-Boc-1-guanylpyrazole (47 mg, 0.15 mmol) in a mixture of THF (1 mL) and water (0.2 mL), a 1 M aqueous LiOH solution (0.2 mL, 0.2 mmol) and triphenylphosphine (79 mg, 0.30 mmol) were sequentially added to a stirred solution of compound **8a** (62 mg, 0.10 mmol). The reaction mixture was stirred at room temperature for 48 h and then THF was removed under reduced pressure. The residue was partitioned between aqueous 10% citric acid and EtOAc. The aqueous layer was extracted with EtOAc (3 times) and then the organic layers were combined, washed once with brine and dried over Na_2SO_4. Finally, the crude product was purified by chromatography on a C_{18} reverse phase semi-preparative HPLC column. HPLC eluant conditions: from 45% of H_2O (0.1% TFA) and 55% of CH_3CN to 30% of H_2O (0.1% TFA) and 70% of CH_3CN, flow rate 20 mL/min, 10 min runs. Yield 31% (26 mg, MW 834.01, 0.031 mmol) of pure trifluoroacetate salt of **15a** as an amorphous white solid. *Analytical characterization*: $[\alpha]_D^{20} = -84.2$ (*c* 0.65, MeOH); ^{1}H NMR (400 MHz, $CDCl_3$): δ: 7.60 (m, 2H), 7.50 (m, 1H), 7.30–7.08 (m, 11H), 6.12 (d, *J* = 8.4 Hz, 1H), 4.94 (m, 1H), 4.64 (d, *J* = 7.2 Hz, 1H), 4.54 (m, 1H), 3.77 (m, 2H), 3.54 (m, 1H), 2.87 (m, 1H), 2.34 (m, 1H), 2.30–1.51 (m, 9H), 1.47 (s, 9H), 1.34 (s, 9H), 1.20 (s, 9H), 1.10 (m, 1H), 0.93 (t, *J* = 7.2 Hz, 3H); ^{13}C NMR (100 MHz, $CDCl_3$): δ: 172.4, 171.3, 169.4, 158.1, 156.0, 154.0, 149.0, 142.0, 141.1, 128.7, 128.6, 127.3, 127.2, 126.9, 80.3, 79.5, 79.2, 61.0, 58.9, 56.8, 56.4, 53.6, 53.5, 40.0, 34.2, 33.3, 32.0, 31.2, 28.3, 27.9, 25.5, 21.0, 10.2. ESI-MS: *m*/*z* 834.2 $[M+H]^+$.

4.1.7. General procedure F—synthesis of compounds 17

$NaBH(OAc)_3$ (26 mg, 0.13 mmol) was added to a stirred solution of compound **9a** (0.10 mmol) and of a carbonyl compound (0.11 mmol) in dry CH_2Cl_2 (2 mL) under nitrogen atmosphere. The reaction mixture was stirred overnight at room temperature, and then the solvent was removed under reduced pressure. The

crude product was purified either by chromatography on a C_{18} reverse phase semi-preparative HPLC column or by Biotage™.

4.1.7.1. Compound 17a. Compound **17a** was synthesized by general procedure F. HPLC eluant conditions: from 80% of H_2O (0.1% NH_3) and 20% of CH_3CN to 20% of H_2O (0.1% NH_3) and 80% of CH_3CN. Yield 79% (49 mg, MW 619.79, 0.079 mmol) of pure **17a** as an amorphous white solid. *Analytical characterization*: $[\alpha]_D^{20} = -88.7$ (*c* 1.08, $CHCl_3$); ^{1}H NMR (400 MHz, $CDCl_3$): 8.60 (d, *J* = 7.2 Hz, 1H), 8.53 (br s, 1H), 7.84 (d, *J* = 8.8 Hz, 1H), 7.40–7.20 (m, 10H), 6.21 (d, *J* = 8.4 Hz, 1H), 5.04 (d, *J* = 6.4, 1H), 4.73 (d, *J* = 7.2 Hz, 1H), 4.61 (t, *J* = 8.4 Hz, 1H), 4.08 (dd, *J* = 13.6, 6.8 Hz, 1H), 3.82 (dd, *J* = 17.2, 8.8 Hz, 1H), 3.00 (m, 2H), 2.80 (m ,1H), 2.64 (br d, *J* = 12.8 Hz, 1H), 2.43 (m, 1H), 2.22 (m, 1H), 1.95–1.60 (m, 8H), 1.45 (s, 9H), 1.31 (t, *J* = 7.2 Hz, 3H), 1.15 (m, 1H), 1.05 (t, *J* = 7.2 Hz, 3H); ^{13}C NMR (100 MHz, $CDCl_3$): 173.8, 170.7, 169.5, 142.1, 128.7, 128.5, 127.4, 127.2, 80.3, 61.2, 58.5, 57.0, 56.5, 54.5, 51.8, 44.7, 38.0, 34.4, 33.2, 32.8, 28.1, 25.7, 12.2, 10.3. ESI-MS: *m*/*z* 620.8 $[M+H]^+$.

Full analytical characterization of compound **17b** is reported in the Supplementary data.

4.1.8. General procedure G—synthesis of compounds 19

$NaBH(OAc)_3$ (26 mg, 0.13 mmol) and acetic acid (6 μL, 0.1 mmol) were sequentially added to a stirred solution of secondary amines **17** (0.10 mmol) and of a carbonyl compound (0.11 mmol) in dry CH_2Cl_2 (2 mL) under nitrogen atmosphere. The reaction mixture was stirred overnight at room temperature, and then the solvent was removed under reduced pressure. The crude product was purified by Biotage™.

4.1.8.1. Compound 19a. Compound **19a** was synthesized by general procedure G, starting from secondary amine **17b**. Biotage™ eluant conditions: from 1% of MeOH and 99% of CH_2Cl_2 to 10% of MeOH and 90% of CH_2Cl_2. Yield 92% (64 mg, MW 695.89, 0.092 mmol) of pure **19a** as an amorphous white solid. *Analytical characterization*: $[\alpha]_D^{20} = -84.2$ (*c* 1.36, $CHCl_3$); ^{1}H NMR (400 MHz, $CDCl_3$): *δ*: 9.10 (br s, 1H), 8.35 (br s, 1H), 7.40–7.00 (m, 15H), 6.21 (d, *J* = 8.4 Hz, 1H), 5.15 (d, *J* = 7.6 Hz, 1H), 4.79 (d, *J* = 7.2 Hz, 1H), 4.49 (dd, *J* = 9.2, 6.0 Hz, 1H), 4.03 (m, 1H), 3.93 (dd, *J* = 17.6, 9.2 Hz, 1H), 3.60 (br s, 1H), 3.29 (br s, 1H), 2.63 (br s, 1H), 2.47 (m, 1H), 2.26 (m, 2H), 2.16 (br s, 3H), 1.95–1.85 (m, 5H), 1.80–1.50 (m, 3H), 1.44 (s, 9H), 1.25 (m, 1H), 0.92 (t, *J* = 7.6 Hz, 3H); ^{13}C NMR (100 MHz, $CDCl_3$): *δ*: 172.2, 170.0, 142.2, 141.3, 128.6, 128.5, 128.4, 127.3, 127.2, 127.1, 79.6, 61.1, 58.3, 56.8, 35.0, 33.6, 33.4, 31.2, 28.4, 26.7, 25.5, 9.9. ESI-MS: *m*/*z* 696.6 $[M+H]^+$.

Full analytical characterization of compounds **19b**,**c** is reported in the Supplementary data.

4.1.8.2. Synthesis of 21a. *N*-Boc glycine (18 mg, 0.10 mmol), EDC·HCl (23 mg, 0.12 mmol), HOBt (16 mg, 0.12 mmol) and dry DIPEA (70 μL, 0.40 mmol) were sequentially added to a stirred solution of **9a** (59 mg, 0.10 mmol) in dry CH_2Cl_2 (2 mL) under nitrogen atmosphere. The reaction mixture was stirred at room temperature overnight and then, after reaction completion, the solvent was removed under reduced pressure. The crude product was taken up with CH_2Cl_2 and then washed once with saturated aqueous NH_4Cl, with saturated aqueous $NaHCO_3$ and with brine. The organic layer was dried over Na_2SO_4, the solvent was removed under reduced pressure and the crude product was purified by Biotage™. Biotage™ eluant conditions: from 1% of MeOH and 99% of CH_2Cl_2 to 10% of MeOH and 90% of CH_2Cl_2. Yield 89% (67 mg, MW 748.91, 0.089 mmol) of pure **21a** as an amorphous white solid. *Analytical characterization*: $[\alpha]_D^{20} = -41.0$ (*c* 1.50, $CHCl_3$); ^{1}H NMR (400 MHz, $CDCl_3$): *δ*: 7.91 (d, *J* = 7.2 Hz, 1H), 7.55–7.15 (m, 12H), 6.21 (d, *J* = 8.8 Hz, 1H), 5.09 (d, *J* = 7.4, 1H), 4.71 (d, *J* = 7.2 Hz, 1H), 4.53 (t, *J* = 8.0, 1H), 4.04 (q, *J* = 7.2, 1H) , 3.77 (m, 3H), 3.45 (m, 1H), 3.05 (m, 1H), 2.45 (m, 1H), 2.25 (m, 1H), 1.90–1.55 (m, 7H), 1.44 (s, 9H), 1.43 (s, 9H), 1.30–1.05 (m, 2H), 0.98 (t, *J* = 7.6 Hz, 3H); ^{13}C NMR (100 MHz, $CDCl_3$): *δ*: 173.3, 171.6, 169.6, 169.4, 165.7, 156.0, 142.1, 141.2, 128.6, 127.4, 127.3, 80.7, 79.8, 61.1, 58.6, 56.8, 55.5, 54.0, 44.2, 39.8, 34.4, 33.3, 31.9, 28.3, 25.7, 25.5, 10.9. ESI-MS: *m*/*z* 749.5 $[M+H]^+$, 771.6 $[M+Na]^+$.

4.1.9. General procedure H—synthesis of compounds 21b,c

Pyridine (81 μL, 1.0 mmol) and a carboxylic acid chloride RCOCl (0.10 mmol) were sequentially added to a stirred solution of **9a** (59 mg, 0.10 mmol) in dry CH_2Cl_2 (2 mL) under nitrogen atmosphere. The reaction mixture was stirred at room temperature overnight and then, after reaction completion, the solvent was removed under reduced pressure. The crude product was purified by Biotage™.

4.1.9.1. Compound 21b. Compound **21b** was synthesized by general procedure H. Biotage™ eluant conditions: from 1% of MeOH and 99% of CH_2Cl_2 to 10% of MeOH and 90% of CH_2Cl_2. Yield 91% (58 mg, MW 633.78, 0.091 mmol) of pure **21b** as an amorphous white solid. *Analytical characterization*: $[\alpha]_D^{20} = -64.0$ (*c* 1.15, $CHCl_3$); ^{1}H NMR (400 MHz, $CDCl_3$): *δ*: 7.91 (d, *J* = 8.8 Hz, 1H), 7.38–7.27 (m, 10H), 7.19 (d, *J* = 8.4 Hz, 1H) 7.05 (br s, 1H), 6.22 (d, *J* = 8.8 Hz, 1H), 4.98 (d, *J* = 6.4 Hz, 1H), 4.72 (d, *J* = 7.6 Hz, 1H), 4.49 (t, *J* = 8.0 Hz, 1H), 3.97 (dd, *J* = 13.2, 6.0, 1H), 3.80 (m, 1H), 3.55 (m, 1H), 3.05 (d, *J* = 12.0 Hz, 1H), 2.45 (m, 1H), 2.25 (m, 1H), 2.08 (s, 3H), 2.00–1.55 (m, 8H), 1.46 (s, 9H), 1.20–1.00 (m, 1H), 1.00 (t, *J* = 7.6 Hz, 3H); ^{13}C NMR (100 MHz, $CDCl_3$): *δ*: 173.6, 171.7, 170.5, 169.3, 155.9, 142.0, 141.1, 128.6, 127.5, 127.3, 127.2, 80.5, 61.2, 59.0, 57.1, 56.8, 54.1, 53.9, 41.4, 40.2, 34.5, 33.1, 31.9, 28.3, 25.6, 25.2, 23.3, 10.3. ESI-MS: *m*/*z* 634.5 $[M+H]^+$, 656.5 $[M+Na]^+$.

Full analytical characterization of compound **21c** is reported in the Supplementary data.

4.1.10. General procedure I—synthesis of compounds 23

A 0.3 M water solution of K_2CO_3 (1.3 mL, 0.40 mmol) and a sulfonyl chloride RSO_2Cl (0.22 mmol) were added to stirred solutions of compound **9a** (**59** mg, 0.10 mmol) in CH_2Cl_2 (2 mL). The reaction mixture was stirred at room temperature overnight and then, after reaction completion, the solvent was removed under reduced pressure. The crude products were purified by Biotage™.

4.1.10.1. Compound 23a. Compound **23a** was synthesized by general procedure I. Biotage™ eluant conditions: from 1% of MeOH and 99% of CH_2Cl_2 to 10% of MeOH and 90% of CH_2Cl_2. Yield 74% (50 mg, MW 669.83, 0.074 mol) of pure **23a** as an amorphous white solid. *Analytical characterization*: $[\alpha]_D^{20} = -101.0$ (*c* 1.68, $CHCl_3$); ^{1}H NMR (400 MHz, $CDCl_3$): *δ*: 7.74 (d, *J* = 8.4 Hz, 1H), 7.30–7.18 (m, 10H), 7.12 (d, *J* = 7.2 Hz, 1H), 6.13 (d, *J* = 8.8 Hz, 1H), 5.95 (d, *J* = 9.2 Hz, 1H), 4.92 (d, *J* = 6.8 Hz, 1H), 4.63 (t, *J* = 8.0 Hz, 1H), 4.40 (t, *J* = 8.4, 1H), 3.92 (dd, *J* = 13.6, 7.6 Hz, 1H), 3.70 (dd, *J* = 13.6, 8.3, 1H), 3.05 (m, 2H), 2.79 (s, 3H), 2.41 (m, 1H), 2.28 (m, 1H), 1.90–1.55 (m, 8H), 1.37 (s, 9H), 1.15 (m, 1H), 0.91 (t, *J* = 7.2 Hz, 3H); ^{13}C NMR (100 MHz, $CDCl_3$): *δ*: 173.5, 171.2, 171.1, 169.3, 155.8, 142.0, 141.1, 128.7, 127.5, 127.4, 127.3, 127.2, 80.4, 61.3, 58.9, 56.8, 53.5, 45.7, 40.0, 39.8, 34.3, 33.1, 31.7, 28.3, 25.7, 25.4, 10.2. ESI-MS: *m*/*z* 692.5 $[M+Na]^+$.

Full analytical characterization of compound **23b** is reported in the Supplementary data.

4.1.11. General procedure J—synthesis of compounds 25

RNCO or RNCS (neat, 0.12 mmol) and dry DIPEA (21 μL, 0.12 mmol) were added to a stirred solution of **9a** (59 mg, 0.10 mmol) in dry CH_2Cl_2 (2 mL). The reaction mixture was stirred

at room temperature overnight, the solvent was removed under reduced pressure and the crude products were purified by Biotage™.

4.1.11.1. Compound 25a. Compound **25a** was synthesized by general procedure J. Biotage™ eluant conditions: 1% of MeOH and 99% of CH_2Cl_2 to 10% of MeOH and 90% of CH_2Cl_2. Yield 89% (59 mg, MW 662.82, 0.089 mmol) of pure **25a** as an amorphous white solid. *Analytical characterization*: $[\alpha]_D^{20} = -83.3$ (*c* 1.11, $CHCl_3$); ^{1}H NMR (400 MHz, $CDCl_3$): δ: 7.86 (d, *J* = 7.4 Hz, 1H), 7.30–7.18 (m, 9H), 7.08 (d, *J* = 7.2 Hz, 2H), 6.13 (d, *J* = 8.8 Hz, 1H), 5.62 (br s, 1H), 4.93 (d, *J* = 6.8 Hz, 1H), 4.63 (d, *J* = 7.6 Hz, 1H), 4.46–4.37 (m, 2H), 3.89 (dd, *J* = 13.6, 7.6 Hz, 1H), 3.68 (dd, *J* = 17.6, 9.2 Hz, 1H), 3.29 (m, 1H), 3.14 (m, 2H), 3.05 (br d, *J* = 12 Hz, 1H), 2.36 (m, 1H), 2.15 (m, 1H), 1.85–1.71 (m, 5H), 1.65–1.56 (m, 3H), 1.40 (m, 1H),1.36 (s, 9H), 1.05 (t, *J* = 7.2 Hz, 3H), 0.89 (t, *J* = 7.6 Hz, 3H); ^{13}C NMR (100 MHz, $CDCl_3$): δ: 173.1, 172.0, 169.3, 158.4, 156.0, 142.0, 141.3, 128.7, 128.6, 127.5, 127.2, 80.6, 61.2, 58.9, 57.1 56.8, 54.5, 42.6, 40.8, 35.2, 34.5, 33.3, 32.0, 31.5, 28.3, 25.5, 25.6, 15.6, 10.3. ESI-MS: *m*/*z* 663.6 $[M+H]^+$, 685.6 $[M+Na]^+$.

Full analytical characterization of compounds **25b–d** is reported in the Supplementary data.

4.1.12. General procedure K—synthesis of compounds 27

RCONCO or RCONCS (neat, 0.12 mmol) and dry DIPEA (21 μL, 0.12 mmol) were added to a stirred solution of **9a** (59 mg, 0.10 mmol) in dry CH_2Cl_2 (2 mL). The reaction mixtures were stirred at room temperature overnight and then the solvent was removed under reduced pressure. The crude products were purified by Biotage™. *Acyl urea a*: Biotage™ eluant conditions: from 1% of MeOH and 99% of CH_2Cl_2 to 10% of MeOH and 90% of CH_2Cl_2. Yield 83% (61 mg, MW 738.87, 0.083 mmol) of pure *N*-Boc protected acyl urea **a** as an amorphous white solid. *Analytical characterization*: $[\alpha]_D^{20} = -91.1$ (*c* 1.33, $CHCl_3$); ^{1}H NMR (400 MHz, $CDCl_3$): δ: 8.82 (bt, *J* = 6.4 Hz, 1H), 8.66 (br s, 1H), 7.95 (d, *J* = 7.2 Hz, 3H), 7.64 (t, *J* = 7.6 Hz, 1H), 7.53 (d, *J* = 8.0 Hz, 2H), 7.40–7.24 (m, 9H), 7.21 (m, 3H), 6.21 (d, *J* = 8.4 Hz, 1H), 5.57 (d, *J* = 8.8 Hz, 1H), 4.75 (d, *J* = 7.2 Hz, 1H), 4.67 (dd, *J* = 10, 7.6, 1H), 4.20 (br s, 1H), 3.85 (dd, *J* = 16.8, 9.2 Hz, 1H), 3.47 (m, 1H), 3.34 (m, 1H), 2.44 (m, 1H), 2.25 (m, 1H), 2.05–1.85 (m, 3H), 1.80–1.60 (m, 4H), 1.47 (s, 9H), 1.15 (m, 1H), 0.97 (t, *J* = 6.4 Hz, 3H); ^{13}C NMR (100 MHz, $CDCl_3$): δ: 172.9, 171.7, 169.5, 167.7, 153.4, 142.1, 141.2, 133.3, 132.2, 129.0, 128.9, 127.4, 127.3, 127.2, 80.1, 61.0, 58.8, 56.8, 56.4, 54.3, 42.2, 40.7, 34.5, 33.3, 32.3, 28.3, 10.2. ESI-MS: *m*/*z* 739.6 $[M+H]^+$, 761.6 $[M+Na]^+$.

2 M aqueous K_2CO_3 (100 μL, 0.20 mmol) was added to a stirred solution of an *N*-Boc protected acyl(thio)urea (0.10 mmol) in MeOH (2 mL). The reaction mixture was stirred at room temperature overnight. After reaction completion, the solvent was removed under reduced pressure. The residue was dissolved in CH_2Cl_2 and washed once with water. The organic layer was dried over Na_2SO_4, and the solvent was removed under reduced pressure. The crude product was used without further purification.

4.1.12.1. Compound 27a. Compound **27a** was synthesized by general procedure K. Yield 82% (52 mg, MW 634.77, 0.082 mmol) pure **27a** as an amorphous white solid. *Analytical characterization*: $[\alpha]_D^{20} = -76.4$ (*c* 1.10, MeOH); ^{1}H NMR (400 MHz, $CDCl_3$): 7.84 (d, *J* = 8.8 Hz, 1H), 7.27–7.08 (m, 11H), 6.13 (d, *J* = 8.8 Hz, 1H), 4.96 (d, *J* = 7.2 Hz, 1H), 4.64 (d, *J* = 7.2 Hz, 1H), 4.46 (m, 1H), 3.88 (dd, *J* = 14.0, 7.2 Hz, 1H), 3.68 (dd, *J* = 17.6, 9.2 Hz, 1H), 3.17 (m, 1H), 3.06 (m, 1H), 2.36 (m, 1H), 2.16 (m, 1H), 1.81–1.70 (m, 4H), 1.65–1.40 (m, 4H), 1.36 (s, 9H), 1.10–1.00 (m, 1H), 0.91 (t, *J* = 7.2 Hz, 3H); ^{13}C NMR (100 MHz, $CDCl_3$): 173.1, 171.7, 169.3, 158.9, 141.8, 141.2, 128.7, 128.6, 127.6, 127.4, 127.3, 127.2, 80.8, 61.1, 58.9, 57.2, 56.8, 54.6, 43.2, 40.7, 34.5, 33.2, 32.3, 29.7, 28.3, 25.6, 25.2, 10.4. ESI-MS: *m*/*z* 635.1 $[M+H]^+$, 657.1 $[M+Na]^+$.

Full analytical characterization of acyl urea b and of compound **27b** is reported in the Supplementary data.

4.1.13. General procedure L—synthesis of compounds 29

Dry TEA (4.0 equiv) and MsCl (4.0 equiv) were added to stirred solutions of alcohol **7** (1.0 equiv) in dry CH_2Cl_2 under argon. The reaction mixture was stirred at room temperature overnight. After reaction completion, the resulting mixture was diluted with CH_2Cl_2 and washed once with saturated aqueous NH_4Cl. The organic layer was dried over Na_2SO_4, and then the solvent removed under reduced pressure. The crude mesylate was dissolved in dry DMF under argon at room temperature, and then a solution of nBu$_4$NCN (8.0 equiv) in dry DMF was added. The reaction mixtures were heated at 0 °C while stirring. After 40 h the solvent was removed under reduced pressure, the crude product was diluted with CH_2Cl_2 and washed with water. The organic layer was dried over Na_2SO_4, and then the solvent removed under reduced pressure. The crude product was purified by Biotage™.

4.1.13.1. Compound 29a. Compound **29a** was synthesized by general procedure L, starting from alcohol **7a** (711 mg, 1.20 mmol). Biotage™ eluant conditions: from 1% of MeOH and 99% of CH_2Cl_2 to 10% of MeOH and 90% of CH_2Cl_2. Yield 51% (368 mg, MW 601.74, 0.612 mmol) of pure **29a** as an amorphous white solid. *Analytical characterization*: $[\alpha]_D^{20} = -69.7$ (*c* 1.19, $CHCl_3$); ^{1}H NMR (400 MHz, $CDCl_3$): δ: 7.82 (d, *J* = 8.8 Hz, 1H), 7.40–7.15 (m, 11H), 6.24 (d, *J* = 8.8 Hz, 1H), 4.98 (br d, *J* = 7.2 Hz, 1H), 4.75 (d, *J* = 7.6 Hz, 1H), 4.54 (dd, *J* = 10.0, 8.0 Hz, 1H), 4.01 (m, 1H), 3.84 (dd, *J* = 17.6, 9.2 Hz, 1H), 2.65 (m, 1H), 2.45 (m, 1H), 2.35–2.10 (m, 3H), 2.15 (m, 1H), 2.00–1.55 (m, 5H), 1.48 (m, 10H), 1.15 (m, 1H), 0.93 (t, *J* = 7.2 Hz, 3H); ^{13}C NMR (100 MHz, $CDCl_3$): δ: 173.0, 170.5, 169.2, 142.1, 141.0, 128.8, 128.6, 127.8, 127.4, 127.3, 127.2, 80.4, 61.0, 58.8, 56.8, 54.2, 37.7, 34.4, 34.0, 33.2, 28.3, 27.9, 26.0, 25.5, 25.2, 20.7, 10.3. ESI-MS: *m*/*z* 602.5 $[M+H]^+$, 624.5 $[M+Na]^+$.

Full analytical characterization of compound **29b** is reported in the Supplementary data.

4.1.14. General procedure M—synthesis of compounds 30

Nitriles **29** were converted to the corresponding amines **30** by continuous flow hydrogenation using the H-Cube™ system (Thales Nanotechnology). 1 M aqueous citric acid (10% of EtOH) was added to nitrile **29** (1 equiv) in EtOH (0.1 M concentration for **29**), and the solution was flowed through a Raney Nickel catalyst cartridge (hydrogen pressure 60 bar, temperature 60 °C, flow rate 0.5 mL/min). After 3 h, the solvent was removed under reduced pressure. The crude product was used without any further purification, and only an analytical sample was purified (semi-preparative HPLC or Biotage™ C_{18} reverse phase chromatography) and characterized (NMR).

4.1.14.1. Compound 30a. Compound **30a** was synthesized by general procedure M, starting from nitrile **29a** (61 mg, 0.10 mmol). HPLC eluant conditions: from 80% of H_2O (0.1% NH_3) and 20% of CH_3CN to 20% of H_2O (0.1% NH_3) and 80% of CH_3CN. Yield 48% (29 mg, MW 605.77, 0.048 mmol) of pure **30a** as an amorphous white solid. *Analytical characterization*: $[\alpha]_D^{20} = -65.7$ (*c* 1.25, $CHCl_3$); ^{1}H NMR (400 MHz, $CDCl_3$): δ: 7.92 (d, *J* = 8.0 Hz, 1H), 7.51 (d, *J* = 8.0, 1H), 7.40–7.15 (m, 10H), 6.16 (d, *J* = 8.8 Hz, 1H), 5.72 (d, *J* = 7.6 Hz, 1H), 4.67 (d, *J* = 5.6 Hz, 1H), 4.55 (t, *J* = 8.8 Hz, 1H), 4.26 (m, 1H), 3.86 (dd, *J* = 17.6, 9.2 Hz, 1H), 2.69 (m, 1H), 2.41 (m, 1H), 2.22 (m, 2H), 2.00–1.60 (m, 7H), 1.55–1.15 (m, 13H), 1.00 (t, *J* = 7.2 Hz, 3H); ^{13}C NMR (100 MHz, $CDCl_3$): δ: 172.5, 171.3, 170.9, 156.3, 141.4, 128.8, 128.6, 127.6, 127.5, 127.2, 80.0, 61.5, 58.5,

57.4, 56.0, 54.8, 37.0, 35.8, 33.4, 33.2, 32.8, 30.2, 27.0, 26.3, 25.8, 10.2. ESI-MS: *m*/*z* 606.0 $[M+H]^+$, 628.0 $[M+Na]^+$.

Full analytical characterization of compound **30b** is reported in the Supplementary data.

4.1.15. General procedure N—synthesis of compounds 33

$NaNO_2$ (5 equiv) and 50% aqueous citric acid (0.5 mL) were sequentially added to a stirred solution of primary amine **30** (1 equiv) in THF (0.3 M concentration for **30**) at 0 °C. The reaction mixture was stirred at room temperature overnight. After reaction completion, the resulting mixture was diluted with water and extracted with EtOAc (3 times). The combined organic layers were dried over Na_2SO_4 and the solvent was removed under reduced pressure. The crude product was purified by semi-preparative HPLC.

4.1.15.1. Compound 33a. Compound **33a** was synthesized by general procedure N, starting from **30a** (183 mg, 0.30 mmol). HPLC eluant conditions: from 80% of H_2O, 20% of CH_3CN and 0.2% AcOH to 100% of CH_3CN and 0.2% AcOH. Yield 16% (28 mg, MW 606.75, 0.048 mmol) of pure **33a** as an amorphous white solid. *Analytical characterization*: ^1H NMR (400 MHz, $CDCl_3$): δ: 8.01 (d, J = 8.9 Hz, 1H), 7.31–7.19 (m, 10H), 7.16 (d, J = 6.9 Hz, 1H), 6.15 (d, J = 8.9 Hz, 1H), 5.09 (d, J = 5.9 Hz, 1H), 4.65 (d, J = 6.9 Hz, 1H), 4.52 (t, J = 8.9 Hz, 1H), 3.90 (br s, 1H), 3.79 (br s, 1H), 3.55 (m, 1H), 3.45 (m, 1H), 2.37 (m, 1H), 2.18 (m, 1H), 1.85–1.50 (m, 8H), 1.37 (s, 9H), 1.32–1.30 (m, 2H), 1.08 (m, 1H), 0.92 (m, 3H); ^{13}C NMR (100 MHz, $CDCl_3$): δ: 172.4, 172.2, 169.6, 142.0, 141.3, 128.6, 128.6, 127.4, 127.3, 80.4, 61.1, 60.9, 58.6, 56.8, 54.9, 37.0, 35.6, 34.7, 34.4, 33.5, 28.3, 25.6, 25.5, 10.3. ESI-MS: *m*/*z* 607.4 $[M+H]^+$, 629.4 $[M+Na]^+$.

Full analytical characterization of compound **33b** is reported in the Supplementary data.

4.1.16. General procedure O—synthesis of compounds 35

Dry DIPEA (1.2 equiv) was added to a solution of primary amine **30** (1 equiv) in dry CH_2Cl_2 (0.1 M concentration in **30**) under argon atmosphere at room temperature. After stirring for 10 min, the solution was treated with benzoyl chloride (1.2 equiv) and dry DIPEA (1.2 equiv). After 1 h, the solution was diluted with CH_2Cl_2 and washed once with water. The organic layer was dried over Na_2SO_4, filtered and concentrated under reduced pressure. The crude product was purified by semi-preparative HPLC.

4.1.16.1. Compound 35a. Compound **35a** was synthesized by general procedure O, starting from **30a** (69 mg, 0.113 mmol). HPLC eluant conditions: from 50% of H_2O, 50% of CH_3CN and 0.2% AcOH to 40% H_2O, 60% of CH_3CN and 0.2% AcOH. Yield 50% (40 mg, MW 709.87, 0.056 mmol) of pure **35a** as an amorphous white solid. *Analytical characterization*: ^1H NMR (400 MHz, $CDCl_3$): δ: 7.93 (d, J = 8.0 Hz, 1H), 7.82 (d, J = 8.0 Hz, 2H), 7.46–7.17 (m, 15H), 6.22 (d, J = 8.0 Hz, 1H), 5.13 (d, J = 8.0 Hz, 1H), 4.72 (d, J = 7.2 Hz, 1H), 4.65 (t, J = 9.2 Hz, 1H), 4.02 (m, 1H), 3.85 (m, 1H), 3.38 (m, 2H), 2.44–2.40 (m, 1H), 2.26–2.21 (m, 1H), 1.88–1.40 (m, 9H), 1.35 (s, 9H), 1.19 (m, 1H), 0.99 (t, J = 7.2 Hz, 3H); ^{13}C NMR (100 MHz, $CDCl_3$): 172.3, 172.2, 169.5, 167.5, 156.1, 141.9, 141.2, 134.7, 131.1, 128.8, 128.7, 128.6, 128.3, 127.5, 127.4, 127.3, 127.2, 127.1, 79.9, 60.9, 58.6, 56.7, 56.6, 54.6, 38.1, 37.7, 34.3, 33.6, 33.4, 32.3, 28.3, 25.7, 25.5, 10.4. ESI-MS: *m*/*z* 710.5 $[M+H]^+$.

Full analytical characterization of compound **35b** is reported in the Supplementary data.

4.1.17. General procedure P—synthesis of compounds 37

A solution of primary amine **30** (1 equiv) and dry DIPEA (1.2 equiv) in dry CH_2Cl_2 (0.1 M concentration in **30**) under argon atmosphere was treated with benzyl isocyanate (1.2 equiv) while stirring at room temperature. After 1 h, the solution was diluted with CH_2Cl_2 and washed once with water. The organic layer was dried over Na_2SO_4 and concentrated under reduced pressure. The crude product was purified by flash chromatography or by Biotage™ C_{18} reverse phase chromatography.

4.1.17.1. Compound 37a. Compound **37a** was synthesized by general procedure P, starting from **30a** (73 mg, 0.120 mmol). Eluant mixture: EtOAc/MeOH 99: 1. Yield 34% (30 mg, MW 738.91, 0.040 mmol) of pure **37a** as an amorphous white solid. *Analytical characterization*: ^1H NMR (400 MHz, $CDCl_3$): δ: 7.94 (d, J = 8.0 Hz, 1H), 7.32–7.16 (m, 15H), 6.20 (d, J = 8.0 Hz, 1H), 5.30–5.12 (m, 2H), 4.73 (d, J = 4.0 Hz, 1H), 4.57 (dd, J = 8.4 Hz, 1H), 4.33 (m, 2H), 4.13 (m, 1H), 3.82 (m, 1H), 3.07 (m, 1H), 1.80–1.78 (m, 5H), 1.61–1.27 (m, 8H), 1.34 (s, 9H), 0.93 (t, J = 6.4 Hz, 3H); ^{13}C NMR (400 MHz, $CDCl_3$): δ: 172.3, 171.9, 170.0, 158.5, 156.2, 141.6, 141.3, 139.8, 128.8, 128.6, 128.5, 128.4, 127.5, 127.4, 127.3, 127.2, 127.0, 80.0, 60.9, 58.4, 56.8, 56.1, 54.8, 44.2, 38.0, 37.1, 33.5, 33.4, 32.8, 32.5, 28.2, 26.2, 26.0, 10.2. ESI-MS: *m*/*z* 739.4 $[M+H]^+$.

Full analytical characterization of compound **37b** is reported in the Supplementary data.

4.1.18. General procedure Q—synthesis of compounds 39

A solution of primary amine **30** (1 equiv) and $NaBH_3CN$ (10 equiv) in dry THF (0.1 M concentration for **30**) under argon atmosphere was treated with dry DIPEA (1.2 equiv) and, a few minutes after, with an aldehyde (1.05 equiv) while stirring at room temperature. After 18 h, the solution was concentrated under reduced pressure and the crude product was purified by semi-preparative HPLC.

4.1.18.1. Compound 39a. Compound **39a** was synthesized by general procedure Q,starting from **30a** (44 mg, 0.072 mmol).. HPLC eluant conditions: from 80% of H_2O, 20% of CH_3CN and 0.2% AcOH to 55% H_2O, 45% of CH_3CN and 0.2% AcOH. Yield 27% (13 mg, MW 693.87, 0.019 mmol) of pure acetate salt of **39a** as an amorphous white solid. *Analytical characterization*: ^1H NMR (400 MHz, $CDCl_3$): 7.75 (br s, 1H), 7.51 (br s, 1H), 7.33–7.22 (m, 10H), 6.21 (d, J = 8.0 Hz, 1H), 5.41 (br s, 1H), 4.72–4.65 (m,1H), 4.56 (m, 1H), 4.03 (br s, 1H), 3.84 (m 1H), 3.01–2.80 (m, 2H), 2.39 (m, 1H), 2.27 (m, 1H), 1.87–1.65 (m, 9H), 1.45 (s, 9H), 1.36–1.10 (m, 5H), 0.90 (br s, 3H); ^{13}C NMR (100.6 MHz, $CDCl_3$): 175.4, 172.7, 171.6, 169.6, 159.6, 141.9, 141.0, 128.7, 128.6, 127.5, 127.4, 127.3, 127.2, 80.6, 61.0, 58.6, 56.9, 56.4, 54.4,45.7, 43.0, 37.2, 34.1, 33.3, 29.7, 29.3, 28.4, 26.0, 25.1, 20.9, 11.2, 10.5. ESI-MS: 634.3 ($M+H^+$), 656.2 ($M+Na^+$)

Full analytical characterization of compounds **39b–d** is reported in the Supplementary data.

4.1.19. General procedure R—synthesis of compounds 3a–40d

A 3 N solution of HCl in MeOH (50 equiv) was added to a stirred solution of *N*-Boc protected compounds **3a–40d** (varying amounts, ranging between 0.018 and 0.090 mmol) in MeOH (0.1 M in *N*-Boc protected compound), except for compounds **3b**, **12a** and **12b**. The reaction mixture was left stirring at room temperature overnight and then concentrated under reduced pressure. When the crude was not sufficiently pure, the residue was purified by chromatography on a C_{18} reverse phase semi-preparative HPLC column and then lyophilized.

4.1.19.1. Compound 3a. Compound **3a** was synthesized by general procedure R from **7a** (30 mg, 0.050 mmol). HPLC eluant conditions: from 80% of H_2O (0.1% TFA) and 20% of CH_3CN to 40% of H_2O (0.1% TFA) and 60% of CH_3CN, flow rate 20 mL/min, 10 min runs. Yield 73% (22 mg, MW 606.63, 0.036 mmol) of pure trifluoroace-

tate salt of **3a** as an amorphous white solid. *Analytical characterization*: $[\alpha]_D^{20} = -52.6$ (*c* 0.46, H_2O); ^1H NMR (400 MHz, D_2O): δ: 7.34–7.28 (m, 10H), 6.05 (s, 1H), 4.65 (m, 1H), 4.54 (m, 1H), 4.01 (m, 1H), 3.85 (m, 1H), 2.25–1.50 (m, 11H), 0.91 (t, *J* = 7.5 Hz, 3H); ^{13}C NMR (100 MHz, D_2O): δ: 173.0, 171.1, 169.5, 141.0, 140.8, 128.7, 127.8, 127.4, 127.2, 63.2, 62.0, 58.4, 57.4, 54.0, 53.8, 39.0, 32.3, 31.1, 29.3, 27.9, 24.4, 8.5. ESI-MS: *m*/*z* 493.6 $[M+H]^+$, 615.6 $[M+Na]^+$.

Full analytical characterization of compounds **4a**,**10a–b**,**14a**, **16a**,**18a–b**,**20a–c**,**22a–c**,**24a–b**,**26a–d**,**28a–b**,**31a**,**32a–b**,**34a–b**,**36a–b**,**38a–b**,**40a–d** is reported in the Supplementary data.

4.1.19.2. Synthesis of 3b. Formic acid (1 mL) was added to **7b** (50 mg, 0.082 mmol). The reaction mixture was stirred at room temperature overnight and then concentrated under reduced pressure. The crude product was treated with 1 M NH_3 in MeOH (2 mL), the reaction mixture was stirred at room temperature overnight and then concentrated under reduced pressure. The residue was purified by semi-preparative HPLC. HPLC eluant conditions: from 80% of H_2O (0.1% HCOOH) and 20% of CH_3CN (0.1% HCOOH) to 60% of H_2O (0.1% HCOOH) and 40% of CH_3CN (0.1% HCOOH), flow rate 20 mL/min, 10 min runs. Yield 74% (20 mg, MW 552.66, 0.036 mmol) of pure formate salt of **3b** as an amorphous white solid. *Analytical characterization:* $[\alpha]_D^{20} = -83.3$ (*c* 1.00, MeOH); *H NMR* (400 MHz, D_2O): δ: 7.40–7.28 (m, 10H), 6.06 (s, 1H), 4.69 (m, 1H), 4.55 (dd, *J* = 5.5, 8.3 Hz, 1H), 4.06 (m, 1H), 3.90 (dd, *J* = 5.3, 7.2 Hz, 1H), 3.59 (d, *J* = 4.9 Hz, 2H), 2.68 (s, 3H), 2.26 (m, 1H), 2.19 (m, 1H), 2.00–1.80 (m, 6H), 1.80–1.55 (m, 3H), 0.98 (t, *J* = 7.2 Hz, 3H); ^{13}C NMR (100 MHz, D_2O): δ: 173.0, 170.9, 168.3, 141.0, 140.8, 129.0, 128.9, 127.4, 127.2, 65.0, 63.2, 62.8, 62.0, 58.7, 57.7, 54.5, 38.9, 32.3, 31.5, 31.0, 29.2, 28.0, 23.4, 8.2. ESI-MS: *m*/*z* 507.4 $[M+H]^+$, 529.4 $[M+Na]^+$.

4.1.19.3. Synthesis of 4b. Azide **10b** was converted to the corresponding amine **4b** by continuous flow hydrogenation using the H-Cube™ system (Thales Nanotechnology). 1 M HCl (107 μL, 0.107 mmol) was added at room temperature to **10b** (61 mg, MW 568.11, 0.107 mmol) in 1:1 water/dioxane (21.4 mL), and the solution was flowed through a Pd–C catalyst cartridge (hydrogen pressure 1 bar, temperature 25 °C, flow rate 1.0 mL/min). The solvent was then evaporated under reduced pressure and the crude product was purified by semi-preparative HPLC. HPLC eluant conditions: from 80% of H_2O (0.2% trifluoroacetic acid) and 20% of CH_3CN (0.2% trifluoroacetic acid) to 60% of H_2O (0.2% trifluoroacetic acid) and 40% of CH_3CN (0.2% trifluoroacetic acid). Yield 32% (25.5 mg, MW 733.7, 0.027 mmol) of pure bis-trifluoroacetate salt of **4b** as an amorphous white solid. *Analytical characterization*: ^1H NMR (400 MHz, D_2O): δ: 7.40–7.21 (m, 10H), 5.70 (s, 1H), 4.65–4.61 (m, 1H), 4.52–4.43 (m, 1H), 4.09–3.98 (m, 1H), 3.94–3.85 (m, 1H), 3.14–3.05 (d, *J* = 12.0 Hz, 1H), 2.91–2.80 (dd, *J* = 12.0, 11.2 Hz, 1H), 2.62 (s, 3H), 2.24–1.79 (m, 8H), 1.78–1.53 (m, 3H), 0.88 (t, *J* = 6.4 Hz, 3H); ^{13}C NMR (100.6 MHz, D_2O): δ: 172.9, 169.2, 169.0, 140.9, 140.7, 129.0, 128.9, 127.8, 127.4, 127.2, 62.6, 61.9, 58.4, 57.8, 54.3, 40.7, 36.1, 32.2, 31.5, 29.9, 28.3, 28.1, 23.3, 8.1. ESI-MS: *m*/*z* 506.3 $[M+H]^+$, 528.3 $[M+Na]^+$.

4.1.20. General procedure S—synthesis of compounds 12

TFA (450 μL, 5.0 mmol) was added to a stirred solution of *N*-Boc esters **11** (0.10 mmol) in CH_2Cl_2 (2 mL). The reaction mixture was stirred at room temperature overnight and then concentrated under reduced pressure. When the crude was not sufficiently pure, the residues were purified by semi-preparative HPLC.

4.1.20.1. Compound 12a. Compound **12a** was synthesized by general procedure S from **11a** (33 mg, 0.052 mmol). HPLC eluant conditions: from 70% of H_2O (0.1% trifluoroacetic acid) and 30% of CH_3CN to 40% of H_2O (0.1% trifluoroacetic acid) and 60% of CH_3CN. Yield 50% (17 mg, MW 648.67, 0.026 mmol) of pure trifluoroacetate salt of **12a** as an amorphous white solid. *Analytical characterization:* $[\alpha]_D^{20} = -43.8$ (*c* 0.68, H_2O); ^1H NMR (400 MHz, D_2O): δ: 7.40–7.26 (m, 10H), 6.02 (s, 1H), 4.71 (m, 1H), 4.51 (dd, *J* = 7.2, 6.0 Hz, 1H), 4.11 (dd, *J* = 11.0, 5.4 Hz, 1H), 4.06–3.96 (m, 2H), 2.21 (m, 1H), 2.13 (m, 1H), 2.03 (s, 3H), 2.00–1.65 (m, 9H), 1.57 (m, 1H), 0.96 (t, *J* = 7.6 Hz, 3H); ^{13}C NMR (100 MHz, D_2O) δ: 175.0, 173.0, 170.5, 169.3, 141.0, 140.8, 129.0, 128.9, 127.8, 127.4, 127.2, 66.1, 62.0, 58.8, 57.7, 54.3, 53.6, 37.0, 32.3, 31.0, 29.5, 27.9, 24.4, 20.4, 8.3. ESI-MS: *m*/*z* 535.0 $[M+H]^+$, 557.0 $[M+Na]^+$.

Full analytical characterization of compound **12b** is reported in the Supplementary data.

4.2. Structural methods

4.2.1. Computational methods

A docking protocol has been set up starting from the high resolution crystal structure of the Smac/BIR3 complex (PDB code 1G73)[21] and using the Glide 2.7 (Grid-based Ligand Docking with Energetics)[45] docking tool. Glide uses a hierarchical series of filters to search for possible locations of the ligand in the active-site region of the receptor. The shape and properties of the receptor are represented on a grid by several different sets of fields that provide progressively more accurate scoring of the ligand poses. To begin the Glide calculation an enclosing box and a bounding box are defined starting from the centre of the reference ligand. The starting poses for the ligands to be screened are generated by placing the centre of the ligand in random points of the bounding box. Glide allows torsional flexibility in the ligand and maintains rigid the protein. Conformational flexibility is handled in Glide via an extensive conformational search, augmented by a heuristic screen that rapidly eliminates conformations deemed unsuitable for binding to a receptor. During the docking process, the cycles conformations in the ligands are held fixed, whereas the other dihedral angles are free to rotate. The refined poses are scored using Schrödinger's proprietary GlideScore scoring function. GlideScore is based on ChemScore[46] but includes a steric-clash term and adds buried polar terms to penalize electrostatic mismatches. Representative conformers derived from a conformational search[47] in the free state (MC/EM,[48] AMBER*,[49] with all atom charges option, water GB/SA[50]) were selected as starting conformations for the docking of recently reported Smac mimics[30] and of the new ligands of general formula **I** (see also Fig. 1).

The XIAP BIR3 protein structure was setup for docking as follows. The Chain D from 1G73 was selected and the metal atom was manually assigned as Zn^{2+}. The co-crystallized Smac chain A was truncated at the four initial residues Ala 1-Val 2-Pro 3-Ile 4. Ile 4 was capped as N-methyl amide. Protein-charged groups that were neither located in the ligand-binding pocket nor involved in salt bridges were neutralized using the Schrödinger pprep script. Hydrogens were added using the Schrödinger graphical user interface Maestro and the resulting structure was optimized using the Schrödinger impref script. Docking results were analyzed by comparing the poses with the crystallographic bound AVPI in BIR3. The pose visual inspection was carried out by monitoring binding features such as intermolecular hydrogen bonds and Van der Waals contacts between the ligand and the protein. Analysis of GlideScore and of its contributes was combined to geometrical pose estimation for the selection of ligand representative poses.

4.2.2. NMR—STD methods

All protein/ligand samples were prepared in a 1:90 protein/ligand ratio. Tipically, the final concentration of the samples was 5 mM in Smac mimic and 0.055 mM in proteins, and the final volume was 200 μL. The buffer used for BIR3 and full length XIAP samples was 100 mM NaCl, 10 mM deuterated Tris, 5 mM deuter-

ated DTT in D_2O or H_2O with 10% D_2O, pH 7.3. The buffer used for L-BIR2–BIR3 was 20 mM, 200 mM, 10 mM deuterated DTT in H_2O with 10% D_2O, pH 6.5. ^1H NMR STD experiments were performed at 600 MHz on a Bruker Avance spectrometer. The probe temperature was maintained at 298 K using the STD sequence of the Bruker library. The on-resonance irradiation of the protein was performed at a chemical shift of −0.05 ppm. Off-resonance irradiation was applied at 20 ppm, where no protein signals were visible. Selective presaturation of the protein was achieved by a train of Gauss-shaped pulses of 21.22-ms length each. The total length of the saturation train was 1.91 s.

4.2.3. Crystallographic methods

Crystals of the different XIAP BIR3 complexes were grown by vapour diffusion methods as co-crystallizations.[36,37] The crystal structures of the XIAP BIR3 complexes with compounds **3a**, **4a** and **24a** were solved by molecular replacement and refined at 2.7 Å, 2.5 Å and 3.0 Å, respectively (PDB codes 3CM7, 3CM2, 3EYL) as previously described.[36,37]

4.3. In vitro biology profiling

4.3.1. Fluorescence polarization assay—cloning, expression and purification of human XIAP BIR3

A pET28 vector (Novagen) with the cDNA coding for human XIAP BIR3 domain from residue 241 to 356 was used to transform *Escherichia coli* strain BL21. Protein expression was induced by adding isopropyl-β-D-thiogalactopyranoside (IPTG) to a final concentration of 1 mM and 100 μM zinc acetate (ZnAc) for 3 h at 37 °C. Bacteria grown in 2YT medium plus kanamycin were harvested, resuspended in a buffer containing 50 mM Tris HCl pH 7.5, 200 mM NaCl and protease inhibitors, treated with 100 μg/mL lysozyme for 30 min in ice and then lysed by sonication. After elimination of debris by centrifugation, the recombinant protein was purified using Ni-NTA (His-trap Ffcrude, Ge-Healthcare) followed by gel filtration (Superdex 200, Ge-Healthcare). BIR3-His-tag was eluted with 250 mM imidazole and thereafter stored in 20 mM Tris pH 7.5, 200 mM NaCl and 10 mM Dithiothreitol.

4.3.2. Fluorescence polarization assay—BIR3—saturation binding experiments

Fluorescent polarization experiments were performed in black, flat-bottom 96-well microplates (PBI) and fluorescent polarization was measured by Ultra plate reader (Tecan). Fluorescent-labelled Smac peptide [AbuRPF-K(5-Fam)-NH2] (FITC-SMAC) to a final concentration of 5 nM and increasing concentration of BIR3-His-tag from 0 to 20 μM were added to an assay buffer. The final volume in each well was 125 μL, with the assay buffer consisting of 100 mM potassium phosphate, pH 7.5; 100 μg/mL bovine γ-globulin; 0.02% sodium azide. After a 15 min shaking, the plate was incubated for 3 h at room temperature. Fluorescence polarization was measured at an excitation and emission wavelengths of 485 nm and 530 nm respectively. The equilibrium binding graphs were constructed by plotting millipolarization units (mP) as function of the XIAP BIR3 concentration. Data were analyzed using Prism 4.0 software (Graphpad Software).

4.3.3. Fluorescence polarization assay—BIR3—competitive binding experiments

SMAC-mimic compounds were evaluated for their ability to displace FITC-SMAC probe from recombinant protein. 5 mM of FITC-SMAC, XIAP BIR3-His-tag and serial dilutions of the SMAC-mimic compounds (concentrations ranging from 4 μM to 0.4 nM) were added to each well to a final volume of 125 μL in the assay buffer described above. The concentration of BIR3-His-tag used was 60 nM, able to bind more than 50% of the ligand in the saturation binding experiment. After being mixed for 15 min on a shaker and incubated 3 h at room temperature, fluorescent polarization was measured by Ultra plate reader (Tecan). All SMAC-mimics and the fluorescent peptide were stocked in DMSO.

4.3.4. Fluorescence polarization assay—cloning, expression and purification of human XIAP linker-BIR2–BIR3

A pET28 vector (Novagen) with the cDNA coding for human XIAP from residue 124 to 356 (linker-BIR2–BIR3), coding for BIR2 and BIR3 domains and the linker region preceding BIR2, was used to transform *Escherichia coli* strain BL21. Protein expression was induced by adding isopropyl-β-D-thiogalactopyranoside (IPTG) to a final concentration of 1 mM and 100 μM zinc acetate (ZnAc) for 20 h at 20 °C. Bacteria grown in 2YT medium plus kanamycin were harvested, resuspended in a buffer containing 50 mM Tris HCl pH 7.5, 200 mM NaCl and protease inhibitors, treated with 100 μg/mL lysozyme for 30 min in ice and then lysed by sonication. After elimination of debris by centrifugation, the recombinant protein was purified using Ni-NTA (His-trap Ffcrude, Ge-Healthcare) followed by gel filtration (Superdex 200, Ge-Healthcare). The linker-BIR2–BIR3-His-tag was eluted with 250 mM imidazole and thereafter stored in 20 mM Tris pH 7.5, 200 mM NaCl and 10 mM Dithiothreitol.

4.3.5. Fluorescence polarization assay—linker-BIR2–BIR3—saturation binding experiments

Fluorescent polarization experiments were performed in black, flat-bottom 96-well microplates (PBI) and fluorescent polarization was measured by Ultra plate reader (Tecan). Fluorescent-labelled dimeric Smac peptide SMAC-1F (Nikolovska-Coleska et al., Analyt. Biochem. 374:87, 2008) to a final concentration of 1 nM and increasing concentration of linker-BIR2–BIR3-His-tag from 0 to 2 μM were added to an assay buffer. The final volume in each well was 125 μL, with the assay buffer consisting of 100 mM potassium phosphate, pH 7.5; 100 μg/mL bovine γ-globulin; 0.02% sodium azide. After a 15 min shaking, the plate was incubated for 3 h at room temperature. Fluorescence polarization was measured at an excitation and emission wavelengths of 485 nm and 530 nm respectively. The equilibrium binding graphs were constructed by plotting millipolarization units (mP) as function of the XIAP linker-BIR2–BIR3 concentration. Data were analyzed using Prism 4.0 software (Graphpad Software).

4.3.6. Fluorescence polarization assay—linker-BIR2–BIR3—competitive binding experiments

SMAC-mimic compounds were evaluated for their ability to displace SMAC-1F probe from recombinant protein. 1 nM of SMAC-1F, 3 nM of XIAP linker-BIR2–BIR3-His-tag and serial dilutions of the SMAC-mimic compounds (concentrations ranging from 2 μM to 0.4 nM) were added to each well to a final volume of 125 μL in the assay buffer described above. After being mixed for 15 min on a shaker and incubated 3 h at room temperature, fluorescent polarization was measured by Ultra plate reader (Tecan). All SMAC-mimics and the fluorescent peptide were stocked in DMSO.

4.3.7. Cellular cytotoxicity assays

4.3.7.1. Cytotoxicity—cell lines. Human cell lines MDA-MB-231 (breast epithelial adenocarcinoma), HL-60 (promieloblast cells) and PC-3 (prostate adenocarcinoma cells) were purchased from Istituto Zooprofilattico di Brescia (www.bs.izs.it). Reagents for cell culture were purchased from Sigma, unless otherwise indicated. Cells were grown on Plastic Petri dishes (Falcon) in RPMI 1640 medium supplemented with 2 mM L-glutamine, Penicillin (100 U/mL) /Streptomicin (100 μg/mL), 10% Fetal Bovine Serum. A sub-cultivation ratio of 1:4 was used. Cells were maintained at 37 °C in an atmosphere of 95% air and 5% CO_2.

4.3.7.2. Cytotoxicity—experimental protocols. Cells were seeded in 96-well flat bottom cell culture plates at a density of 5000 cells/well in 100 μL of culture medium. HL-60 cells were immediately stimulated with the indicated compounds for 96 h in the incubator. MDA-MB-231 and PC-3 cells were allowed to adhere for 24 h. prior to be exposed to the compounds for 96 h in the incubator. Cells were exposed to the following concentrations of the compounds: 50 nM, 100 nM, 200 nM, 500 nM, 1 μM, 5 μM, 10 μM, 50 μM and 100 μM. Each point was done in triplicate. The cellular growth inhibitory effect of our compounds was evaluated using the MTT assay (Sigma). After 96 h of treatment, 10 μL of MTT reagent solution (5 mg of MTT powder/mL diluted in Phosphate Buffer Salt saline solution) were added in each well and allowed to react for 3 h in the incubator. After 3 h cells were solubilized in Lysis Buffer (10% SDS/0.1% HCl in water, 100 μL for each well) for 24 h at 37 °C. Finally, the absorbance was measured at 570 nm using a multiplate reader. Absorbance values were collected and IC_{50}/IC_{80} values were determined using GraphPad Prism5 software. The experiments were repeated twice.

4.4. In vitro ADMET profiling

4.4.1. Solubility

Solubility was evaluated at pH 7.4 and at pH 3.0. Standard and sample solutions (250 μM) were prepared from a 10 mM DMSO stock solution using three different solutions: acetonitrile/buffer, acetic acid 50 mM, pH 3 and ammonium acetate buffer 50 mM, pH 7.4, with a final DMSO content of 2.5% (v/v).The 250 μM product suspensions/solutions were prepared directly in Millipore MultiScreen-96 filter plates (0.4 μm PTCE membrane) and sealed. Plates were left for 24 h at room temperature under shaking to achieve 'pseudo-thermodynamic equilibrium' and to pre-saturate the membrane filter. Product suspensions/solutions were then filtered using centrifugation, and analysed with a Waters UPLC/UV/TOF-MS, using UV-detection at 254 nm for quantitation.

4.4.2. Metabolic stability

Stock solution (10 mM DMSO) of test compounds were added to an incubation mixture in a 96-well microplate containing 20 pmol/mL hCYP3A4 (0.1–0.2 mg/mL protein). The mixture was split into two aliquots: one receiving a NADPH regenerating system, one receiving only phosphate buffer. The final substrate concentration was 1 μM along with 0.25% of organic solvent. Incubation proceeded for 1 h at 37 °C and was then stopped by addition of acetonitrile to precipitate proteins. Samples were then analyzed using a Waters UPLC/UV/TOF-MS system. The metabolic stability value was reported as per cent remaining of unchanged compound in incubation with NADPH respect to the incubation mixture without cofactor.

4.4.3. PAMPA permeability

The passive permeability was evaluated using a Parallel Artificial Membrane Permeability Assay (PAMPA). The PAMPA membrane was composed of a mechanical support (96 well plate, 0.45 μM, hydrophobic PVDF, Millipore) onto which was deposited a lipid mixture (porcine polar brain lipids in dodecane 2% w/v). Compounds (10 μM in HBSS + Hepes buffer, pH 7.4) were added to the Donor chamber and incubated (together with a internal standard compound, warfarin, to verify membrane integrity) for 4 h at 37 °C and 80% humidity. Concentrations of Reference, Donor and Acceptor solutions were analyzed using a Waters UPLC/UV/TOF-MS system.

4.4.4. Plasma protein binding

Plasma protein binding was evaluated by equilibrium dialysis in 96-well dialysis plates (Harvard, 10 kDa cut-off). Spiked plasma samples at 10 μM were incubated in triplicate at room temperature for 30 min and then dialysed against the same volume of buffer solution (67 mM, pH 7.4) for 4 h at 37 °C at 20 rpm in a rotating incubator. After dialysis, 3 volumes of acetonitrile were added to precipitate proteins, followed by centrifugation at 4000 rpm for 15 min at 4 °C and dilution with 0.1% HCOOH. LC–ESI(+)-MSMS measurements using a fast gradient were performed using an API4000 triple quadrupole mass spectrometer (Applied Biosystems) in the multiple reaction monitoring mode (MRM). The fraction unbound was calculated as the ratio between the concentration unbound ligand (buffer compartment concentration) and the total concentration (from the denaturation of plasma compartment samples).

Supplementary data

Supplementary data associated with this article can be found, in the online version, at doi:10.1016/j.bmc.2009.07.009.

References and notes

1. Fulda, S.; Debatin, K. M. *Curr. Cancer Drug Targets* **2004**, *4*, 569.
2. Kim, R. *Cancer* **2005**, *103*, 1551.
3. Okouchi, M.; Ekshyyan, O.; Maracine, M.; Aw, T. Y. *Antioxid. Redox Signal.* **2007**, *9*, 1059.
4. Fulda, S.; Debatin, K. M. *Oncogene* **2006**, *25*, 4798.
5. Falschlehner, C.; Emmerich, C. H.; Gerlach, B.; Walczak, H. *Int. J. Biochem. Cell Biol.* **2007**, *39*, 1462.
6. Nguyen, D. M.; Hussain, M. *J. Bioenerg. Biomembr.* **2007**, *39*, 13.
7. Kroemer, G.; Martin, S. J. *Nat. Med.* **2005**, *11*, 725.
8. Liston, P.; Young, S. S.; Mackenzie, A. E.; Korneluk, R. G. *Apoptosis* **1997**, *2*, 423.
9. Danson, S.; Dean, E.; Dive, C.; Ranson, M. *Curr. Cancer Drug Targets* **2007**, *7*, 785.
10. Crook, N. E.; Clem, R. J.; Miller, L. K. *J. Virol.* **1993**, *67*, 2168.
11. Shi, Y. *Protein Sci.* **2004**, *13*, 1979.
12. Srinivasula, S. M.; Ashwell, J. D. *Mol. Cell* **2008**, *30*, 123.
13. Dubrez-Daloz, L.; Dupoux, A.; Cartier, J. *Cell Cycle* **2008**, *7*, 1036.
14. Holcik, M.; Gibson, H.; Korneluk, R. G. *Apoptosis* **2001**, *6*, 253.
15. Mufti, A. R.; Burstein, E.; Duckett, C. S. *Arch. Biochem. Biophys.* **2007**, *463*, 168.
16. Deveraux, Q. L.; Leo, E.; Stennicke, H. R.; Welsh, K.; Salvesen, G. S.; Reed, J. C. *EMBO J.* **1999**, *18*, 5242.
17. Du, C.; Fang, M.; Li, Y.; Li, L.; Wang, X. *Cell* **2000**, *102*, 33.
18. Verhagen, A. M.; Ekert, P. G.; Pakusch, M.; Silke, J.; Connolly, L. M.; Reid, G. E.; Moritz, R. L.; Simpson, R. J.; Vaux, D. L. *Cell* **2000**, *102*, 43.
19. Chai, J.; Du, C.; Wu, J.-W.; Kyin, S.; Wang, X.; Shi, Y. *Nature* **2000**, *406*, 855.
20. Liu, Z.; Sun, C.; Olejniczak, E. T.; Meadows, R. P.; Betz, S. F.; Oost, T.; Herrmann, J.; Wu, J. C.; Fesik, S. W. *Nature* **2000**, *408*, 1004.
21. Wu, G.; Chai, J.; Suber, T. L.; Wu, J. W.; Du, C.; Wang, X.; Shi, Y. *Nature* **2000**, *408*, 1008.
22. Shiozaki, E. N.; Chai, J.; Rigotti, D. J.; Riedl, S. J.; Li, P.; Srinivasula, S. M.; Alnemri, E. S.; Fairman, R.; Shi, Y. *Mol. Cell* **2003**, *11*, 519.
23. Riedl, S. J.; Renatus, M.; Schwarzenbacher, R.; Zhou, Q.; Sun, C.; Fesik, S. W.; Liddington, R. C.; Salvesen, G. S. *Cell* **2001**, *104*, 791.
24. Shi, Z.; Liang, Y. J.; Chen, Z. S.; Wang, X. H.; Ding, Y.; Chen, L. M.; Fu, L. W. *Oncol. Rep.* **2007**, *17*, 969.
25. Mizutani, Y.; Nakanishi, H.; Li, Y. N.; Matsubara, H.; Yamamoto, K.; Sato, N.; Shiraishi, T.; Nakamura, T.; Mikami, K.; Okihara, K.; Takaha, N.; Ukimura, O.; Kawauchi, A.; Nonomura, N.; Bonavida, B.; Miki, T. *Int. J. Oncol.* **2007**, *30*, 919.
26. Dean, E. J.; Ranson, M.; Blackhall, F.; Dive, C. *Expert Opin. Ther. Targets* **2007**, *11*, 1459.
27. Deveraux, Q. L.; Roy, N.; Stennicke, H. R.; Van Arsdale, T.; Zhou, Q.; Srinivasula, S. M.; Alnemri, E. S.; Salvesen, G. S.; Reed, J. C. *EMBO J.* **1998**, *17*, 2215.
28. McCarthy, J. V.; Dixit, V. M. *J. Biol. Chem.* **1998**, *273*, 24009.
29. Bertrand, M. J.; Milutinovic, S.; Dickson, K. M.; Ho, W. C.; Boudreault, A.; Durkin, J.; Gillard, J. W.; Jaquith, J. B.; Morris, S. J.; Barker, P. A. *Mol. Cell* **2008**, *30*, 689.
30. Sun, H.; Nikolovska-Coleska, Z.; Yang, C.-Y.; Xu, L.; Liu, M.; Tomita, Y.; Pan, H.; Yoshioka, Y.; Krajewski, K.; Roller, P. P.; Wang, S. *J. Am. Chem. Soc.* **2004**, *126*, 16686.
31. Sun, H.; Nikolovska-Coleska, Z.; Lu, J.; Qiu, S.; Yang, C.-Y.; Gao, W.; Meagher, J.; Stuckey, J.; Wang, S. *J. Med. Chem.* **2006**, *49*, 7916.
32. Scolastico, C.; Manzoni, L.; Seneci, P.; Belvisi, L.; Delia, D.; Bolognesi, M.; Mastrangelo, E.; Milani, M.; Motto, I.; Drago, C. EPO 7021843, 2007.
33. Scolastico, C.; Manzoni, L.; Colombo, M.; Bracci, A. PCT WO2005042531, 2005.
34. Manzoni, L.; Arosio, D.; Belvisi, L.; Bracci, A.; Colombo, M.; Invernizzi, D.; Scolastico, C. *J. Org. Chem.* **2005**, *70*, 4124.
35. Schrödinger, LLC, New York, First Discovery Suite.
36. Mastrangelo, E.; Cossu, F.; Milani, M.; Sorrentino, G.; Lecis, D.; Delia, D.; Manzoni, L.; Drago, C.; Seneci, P.; Scolastico, C.; Rizzo, V.; Bolognesi, M. *J. Mol. Biol.* **2008**, *384*, 673.

37. Cossu, F.; Mastrangelo, E.; Milani, M.; Sorrentino, G.; Lecis, D.; Delia, D.; Manzoni, L.; Seneci, P.; Scolastico, C.; Bolognesi, M. *Biochem. Biophys. Res. Commun.* **2009**, *378*, 162.
38. Meyer, B.; Peters, T. *Angew. Chem., Int. Ed.* **2003**, *42*, 864.
39. Nikolovska-Coleska, Z.; Wang, R.; Fang, X.; Pan, H.; Tomita, Y.; Li, P.; Roller, P. P.; Krajewski, K.; Saito, N. G.; Stuckey, J. A.; Wang, S. *Anal. Biochem.* **2004**, *332*, 261.
40. Nikolovska-Coleska, Z.; Meagher, J. L.; Jiang, S.; Kawamoto, S. A.; Gao, W.; Yi, H.; Qin, D.; Roller, P. P.; Stuckey, J. A.; Wang, S. *Anal. Biochem.* **2008**, *374*, 87.
41. Li, L.; Thomas, R. M.; Suzuki, H.; De Brabander, J. K.; Wang, X.; Harran, P. G. *Science* **2004**, *305*, 1471.
42. Sun, H.; Nikolovska-Coleska, Z.; Yang, C.-Z.; Qian, D.; Lu, J.; Qiu, S.; Bai, L.; Peng, Y.; Cai, Q.; Wang, S. *Acc. Chem. Res.* **2008**, *41*, 1264.
43. Nikolovska-Coleska, Z.; Meagher, J. L.; Jiang, S.; Yang, C.-Y.; Qiu, S.; Roller, P. P.; Stuckey, J. A.; Wang, S. *Biochemistry* **2008**, *47*, 9811.
44. Peng, Y.; Sun, H.; Nikolovska-Coleska, Z.; Qiu, S.; Yang, C.-Y.; Lu, J.; Cai, Q.; Yi, H.; Kang, S.; Yang, D.; Wang, S. *J. Med. Chem.* **2008**, *51*, 8158.
45. Glide, version 2.7, Schrödinger, LLC, New York, NY.
46. Eldridge, M. D.; Murray, C. W.; Auton, T. R.; Paolini, G. V.; Mee, R. P. *J. Comput Aided Mol. Des.* **1997**, *11*, 425.
47. MACROMODEL, Version 8.5; Schrödinger, LLC: New York, NY.
48. Chang, G.; Guida, W. C.; Still, W. C. *J. Am. Chem. Soc.* **1989**, *111*, 4379.
49. Weiner, S. J.; Kollman, P. A.; Nguyen, D. T.; Case, D. A. *J. Comput. Chem.* **1986**, *7*, 230.
50. Still, W. C.; Tempczyk, A.; Hawley, R. C.; Hendrickson, T. *J. Am. Chem. Soc.* **1990**, *112*, 6127.